MIL-HDBK-776 (AR)

15 September 1981

MILITARY HANDBOOK

SHAFTS, ELASTIC
TORSIONAL STRESS ANALYSIS OF

NO DELIVERABLE DATA
REQUIRED BY THIS DOCUMENT

AREA CDNC

MIL-HDBK-776(AR)
15 September 1981

DEPARTMENT OF DEFENSE
WASHINGTON, DC 20360

Shafts, Elastic Torsional Stress Analysis Of

MIL-HDBK-776(AR)

1. This standardization handbook is approved for use by the Armament Research
and Development Command, Department of the Army, and is available for use by all
departments and agencies of the Department of Defense.

2. Beneficial comments (recommendations, additions, deletions) and any per-
tinent data which may be of use in improving this document should be addressed
to: US Army Armament Research and Development Command, ATTN: DRDAR-TST-S, Dover,
NJ 07801.

MIL-HDBK-776(AR)
15 September 1981

FOREWORD

Design charts and tables have been developed for the elastic torsional stress analyses of free prismatic shafts, splines and spring bars with virtually all common industrially encountered thick cross sections. Circular shafts with rectangular and circular keyways, external splines, and milled flats along with rectangular and X-shaped torsion bars are presented.

A computer program ("SHAFT") was developed which provides a finite difference solution to the governing (POISSON's) partial differential equation which defines the stress functions for solid and hollow shafts with generalized contours. Using the stress function solution for the various shapes, and Prandtl's membrane analogy, dimensionless design charts (and tables) have been generated for transmitted torque and maximum shearing stress. The design data have been normalized for a unit dimension of the cross section (radius or length) and are provided for solid shapes.

The eleven solid shapes presented, along with the classical circular cross section solution, provides the means for analyzing 144 combinations of hollow shafts with various outer and inner contours. Hollow shafts may be analyzed by using the computer program directly or by using the solid shape charts in this paper and the principles of superposition based on the concept of parallel shafts. Stress/torque ratio curves are presented as being more intuitively recognizable and useful than those of stress alone.

Sample problems illustrating the use of the charts and tables as design tools and the validity of the superposition concept are included.

iii

MIL-HDBK-776(AR)
15 September 1981

TABLE OF CONTENTS

Tables

v

MIL-HDBK-776(AR)
15 September 1981

Figures

TORSIONAL ANALYSIS OF SPLINED & MILLED SHAFTS

The elastic stress analysis of uniformly circular shafts in torsion is a familiar and straighforward concept to design engineers. As the bar is twisted, plane sections remain plane, radii remain straight, and each section rotates about the longitudinal axis. The shear stress at any point is proportional to the distance from the center, and the stress vector lies in the plane of the circular section and is perpendicular to the radius to the point, with the maximum stress tangent to the outer face of the bar. The torsional stiffness is a function of material property, angle of twist, and the polar moment of inertia of the circular cross-section. These relationships are expressed as:

$$\Theta = T/J \cdot G, \text{ or } T = G \cdot \Theta \cdot J$$

and $$S_s = T \cdot r/J, \text{ or } S_s = G \cdot \Theta \cdot r$$

Where T = twisting moment or transmitted torque, G = Modulus of Rigidity of the shaft material, Θ = angle of twist per unit length of the shaft, J = polar moment of inertia of the (circular) cross-section, S_s = shear stress, and r = radius to any point.

However, if the cross-section of the bar deviates even slightly from a circle, as in a splined shaft, the situation changes radically and far more complex design equations are required. Sections of the bar do not remain plane, but warp into surfaces, and radial lines through the center do not remain straight. The distribution of shear stress on the section is no longer linear, and the direction of shear stress is not normal to a radius.

The governing partial differential equation, from Saint-Vernant's theory is

$$\frac{\partial^2 \varphi}{\partial X^2} + \frac{\partial^2 \varphi}{\partial Y^2} = -2G\Theta$$

1

MIL-HDBK-776(AR)
15 September 1981

where ϕ = Saint-Venant's torsion stress function. The prob-
lem then is to find a ϕ function which satisfies this equation
and also the boundary conditions that ϕ = a constant along the
boundary. The ϕ function has the nature of a potential func-
tion, such as voltage, hydrodynamic velocity, or gravitational
height. Its absolute value is, therefore, not important; only
relative values or differences are meaningful.

The solutions to this equation required complicated math-
ematics. Even simple, but commonplace, practical cross-sec-
tions could not be easily reduced to manageable mathematical
formulae, and numerical approximations or intuitive methods
had to be used.

One of the most effective numerical methods to solve
for Saint-Venant's torsion stress function is that of finite
differences and the best intuitive method, the membrane ana-
logy, came from Prandtl. He showed that the compatibility
equation for a twisted bar was the "same" as the equation for
a membrane stretched over a hole in a flat plate, then in-
flated. This concept provides a simple way to visualize the
torsional stress characteristics of shafts of any cross-
section relative to those of circular shafts for which an
exact analytical solution is readily obtainable. A computer pro-
gram called SHAFT was written and applied to produce the dimension-
less design charts on the following pages.

The three-dimensional plot of ϕ over the cross-section is
a surface and, with ϕ set to zero (a valid constant) along the
periphery, the surface is a domb or ϕ membrane. The trans-
mitted torque (T) is proportional to twice the volume under the
membrane and the stress (S_s) is proportional to the slope of the
membrane in the direction perpendicular to the measured slope.
Neglecting the stress concentration of sharp re-entrant cor-
ners, which are relieved with generous fillets, the maximum
stress for bars with solid cross sections is at the point on
the periphery nearest the center.

The design data have been normalized for a unit dimension
(radius or length) of the shaft cross-section and are in di-
mensionless format. The data and charts may, therefore, be
used for shafts of any dimensions, materials and twist (loading).

2
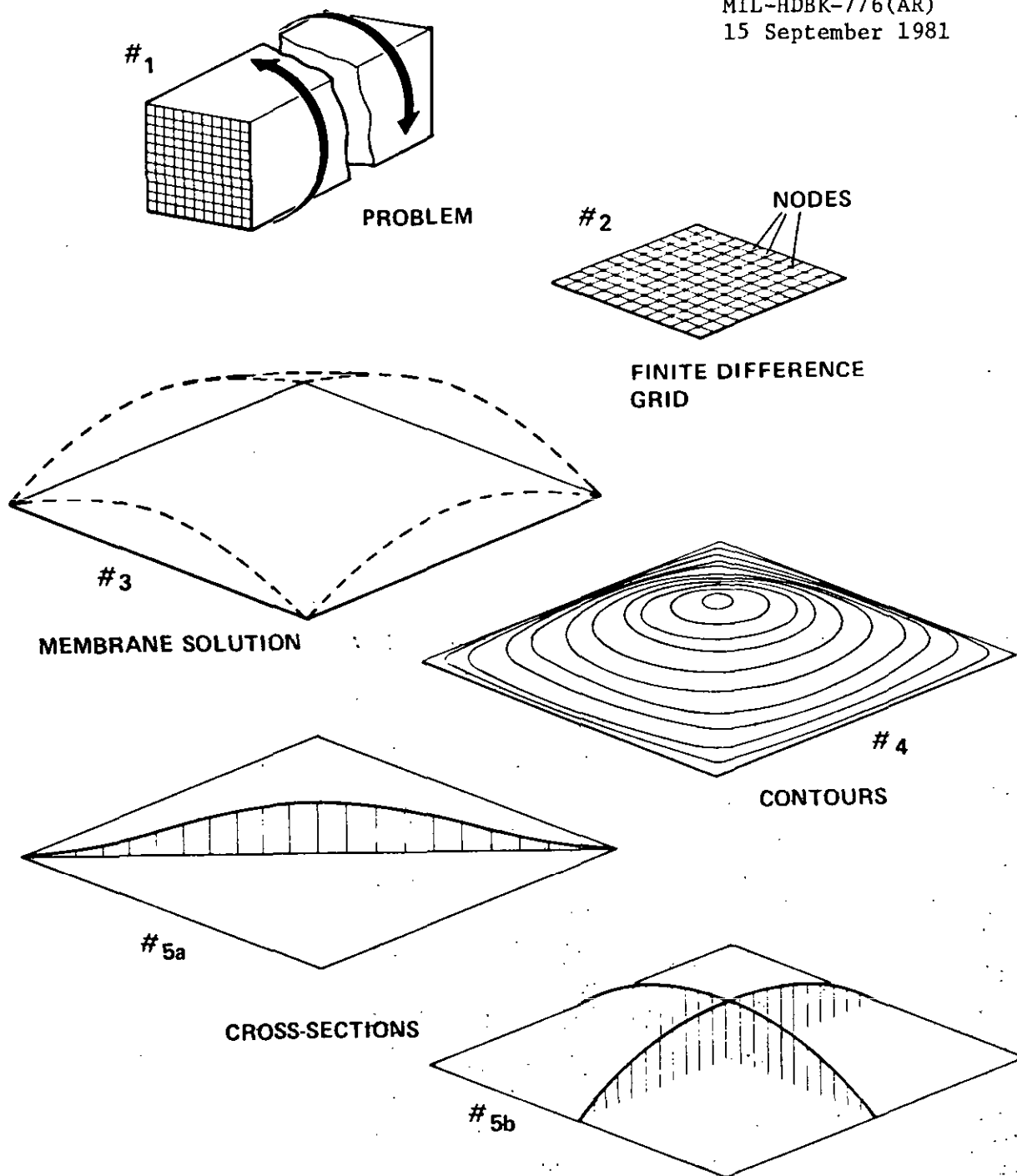
Figure 1. Membrane analogy.

MIL-HDBK-776(AR)
15 September 1981

DESIGN CHARTS AND TABLES

Design charts and related data which support the elastic torsional stress analyses conducted by MISD are shown in figures 2 through 25 and tables 2 through 25, respectively. The item nomenclature used in the analyses is given in table 1.

These data are based on the stress function solution for various shapes provided by the SHAFT computer program and on Prandtl's membrane analogy.

Since the design charts are dimensionless, they can be used for shafts of any material and any dimensions.

4

Table 1. Element nomenclature

TORSIONAL PROPERTIES
OF
SOLID, NON-CIRCULAR SHAFTS
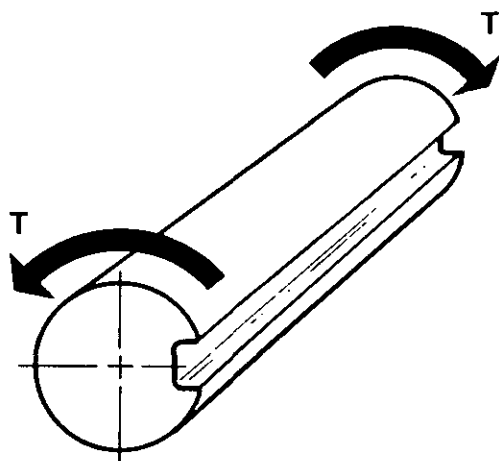
T = TRANSMITTED TORQUE, N · m (lb · in.)

θ = ANGLE OF TWIST PER UNIT LENGTH, rad/mm (rad/in.)

G = MODULUS OF RIGIDITY OR MODULUS OF ELASTICITY IN SHEAR, kPa (lb/in.^{2})

R = OUTER RADIUS OF CROSS-SECTION, mm (in.)

$V, \dfrac{d\phi}{ds}, f$ = VARIABLES FROM CHARTS (OR TABLES) RELATED TO VOLUME UNDER "SOAP FILM MEMBRANE" AND SLOPE OF "MEMBRANE"

S_s = SHEAR STRESS, kPa (lb/in.^{2})

$$T = 2 \cdot G \cdot \theta \, (V) R^4$$

$$S_s = G \cdot \theta \, (\tfrac{d\phi}{ds}) R$$

$$\frac{S_s}{T} = \frac{\frac{d\phi}{ds}}{2 \cdot V \cdot R^3} = f \, (\frac{1}{R^3})$$

5
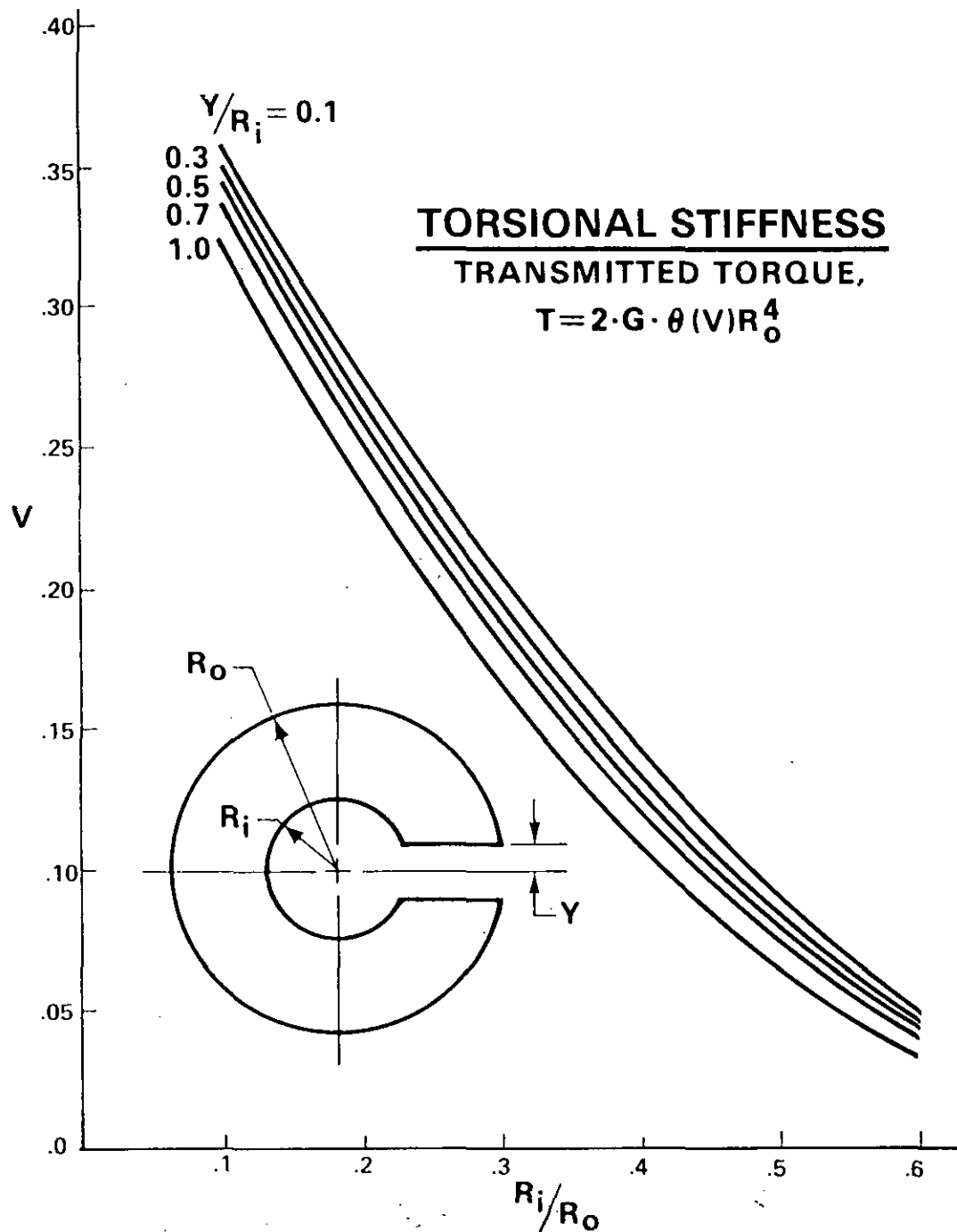
Figure 2. Split shaft, torque.

Table 2. Split shaft, volume factor (V)

Y/Ri	Ri/Ro					
	0.1	0.2	0.3	0.4	0.5	0.6
0.1	.3589	.2802	.2068	.1422	.0891	.0491
0.2	.3557	.2762	.2030	.1391	.0870	.0478
0.3	.3525	.2722	.1991	.1360	.0848	.0464
0.4	.3492	.2680	.1952	.1328	.0825	.0450
0.5	.3457	.2637	.1911	.1294	.0801	.0436
0.6	.3423	.2593	.1869	.1260	.0777	.0421
0.7	.3387	.2548	.1824	.1223	.0750	.0405
0.8	.3350	.2499	.1776	.1183	.0722	.0387
0.9	.3312	.2447	.1725	.1139	.0689	.0367
1.0	.3269	.2389	.1665	.1087	.0649	.0340

SHEAR STRESS

MAXIMUM AT INNER EDGE, AT X

$$S_s = T \left({}^f/R_o^3 \right)$$

$Y/R_i = 1.0$

0.9

0.7

0.5

0.3

0.1

Figure 3. Split shaft, stress.

8
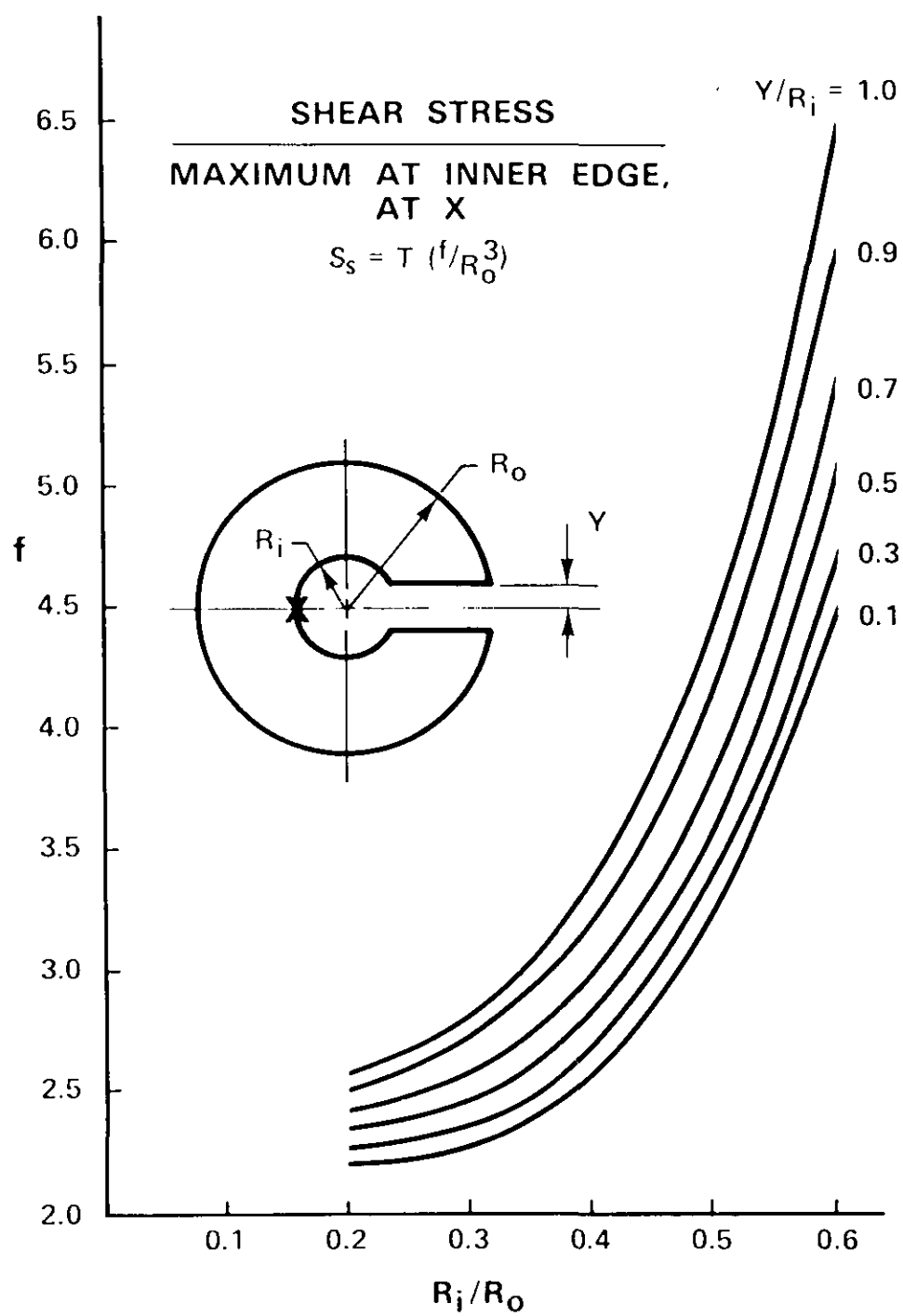
Table 3. Split shaft, stress factor (f)

Y/Ri	Ri/Ro				
	0.2	0.3	0.4	0.5	0.6
0.1	2.2140	2.2742	2.5771	3.2178	4.4650
0.2	2.2447	2.3162	2.6336	3.2977	4.5865
0.3	2.2767	2.3608	2.6942	3.3838	4.7182
0.4	2.3103	2.4082	2.7597	3.4771	4.8620
0.5	2.3461	2.4594	2.8304	3.5795	5.0233
0.6	2.3883	2.5142	2.9084	3.6930	5.2016
0.7	2.4233	2.5750	2.9955	3.8232	5.4082
0.8	2.4670	2.6423	3.0952	3.9744	5.6550
0.9	2.5142	2.7197	3.2141	4.1618	5.9691
1.0	2.5672	2.8140	3.3690	4.4218	6.4392

9

TORSIONAL STIFFNESS

$$\frac{\text{TRANSMITTED TORQUE,}}{}$$

$$T = 2 \cdot G \cdot \theta \, (V) R^4$$
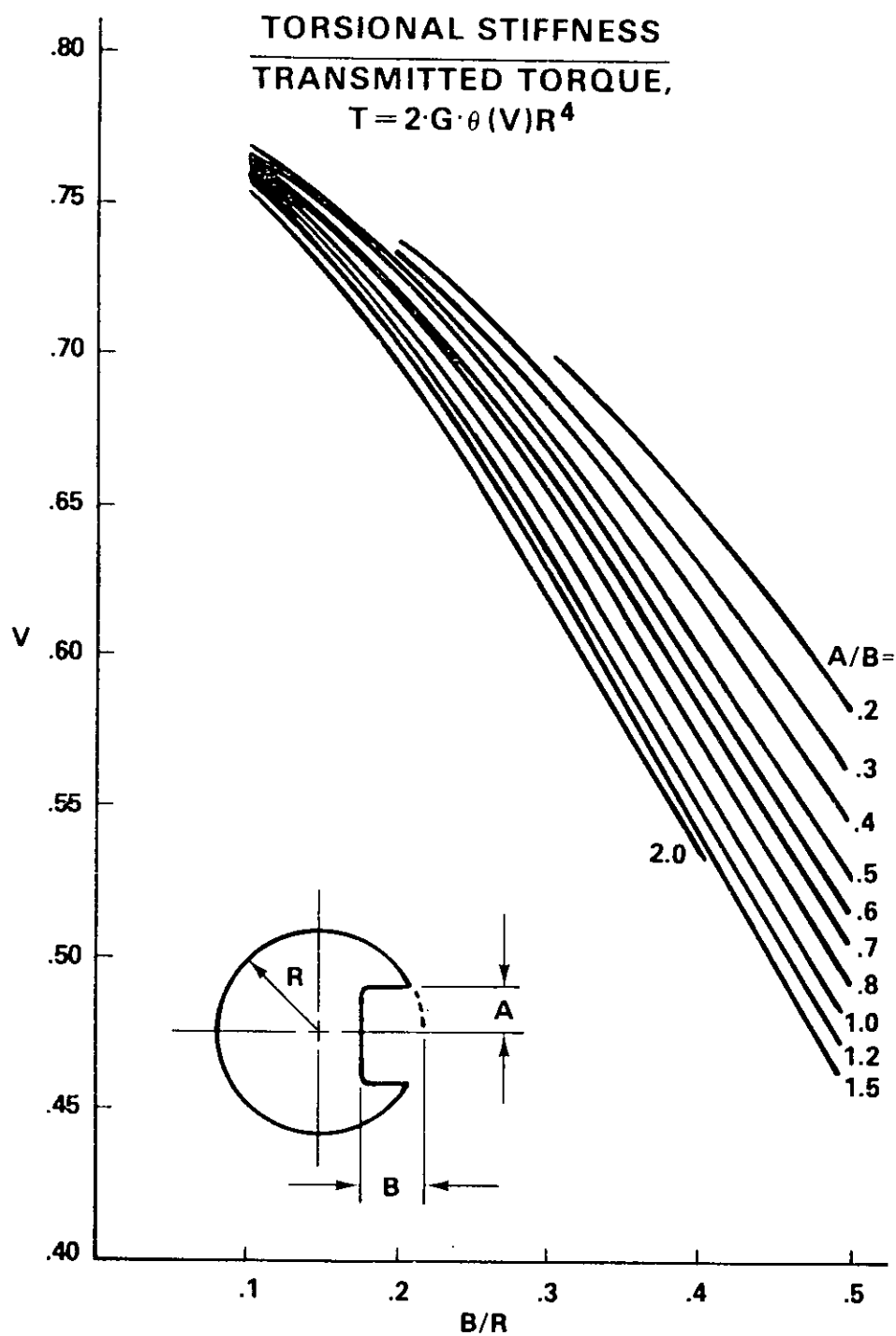
Figure 4. Single keyway shaft, torque.

Table 4. Single keyway shaft, volume factor (V)

A/B	B/R				
	0.1	0.2	0.3	0.4	0.5
0.2			.6994	.6472	.5864
0.3		.7379	.6900	.6316	.5648
0.4		.7341	.6816	.6173	.5459
0.5	.7682	.7290	.6725	.6043	.5294
0.6	.7676	.7262	.6663	.5941	.5152
0.7	.7668	.7224	.6592	.5848	.5032
0.8	.7658	.7190	.6533	.5762	.4931
0.9	.7647	.7162	.6480	.5686	.4849
1.0	.7633	.7125	.6424	.5619	.4783
1.2	.7621	.7079	.6347	.5531	.4697
1.5	.7592	.7012	.6260	.5449	.4649
2.0	.7560	.6945	.6200	.5424	

11
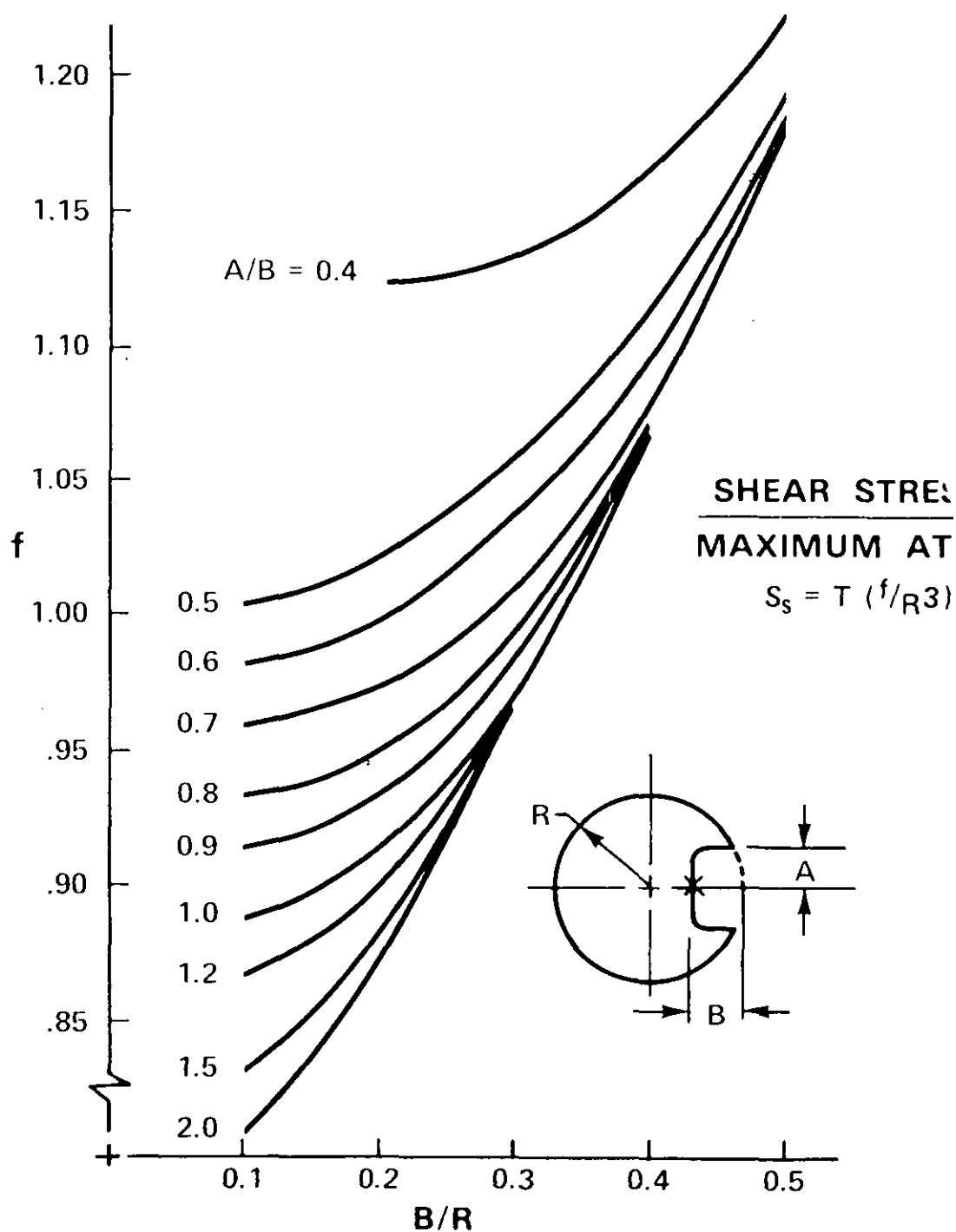
Figure 5.   Single keyway shaft, stress

Table 5. Single keyway shaft, stress factor (f)

A/B	B/R				
	0.1	0.2	0.3	0.4	0.5
0.3		1.1867	1.2273	1.2538	1.2832
0.4		1.1241	1.1333	1.1642	1.2234
0.5	.9899	1.0303	1.0624	1.1155	1.1962
0.6	.9767	1.0077	1.0387	1.0960	1.1859
0.7	.9602	.9746	1.0098	1.0820	1.1848
0.8	.9393	.9466	.9953	1.0737	1.1885
0.9	.9124	.9334	.9843	1.0699	1.1944
1.0	.8773	.9131	.9749	1.0691	1.2009
1.2	.8651	.8993	.9684	1.0721	1.2120
1.5	.8300	.8829	.9655	1.0774	1.2198
2.0	.8083	.8752	.9667	1.0799	

13
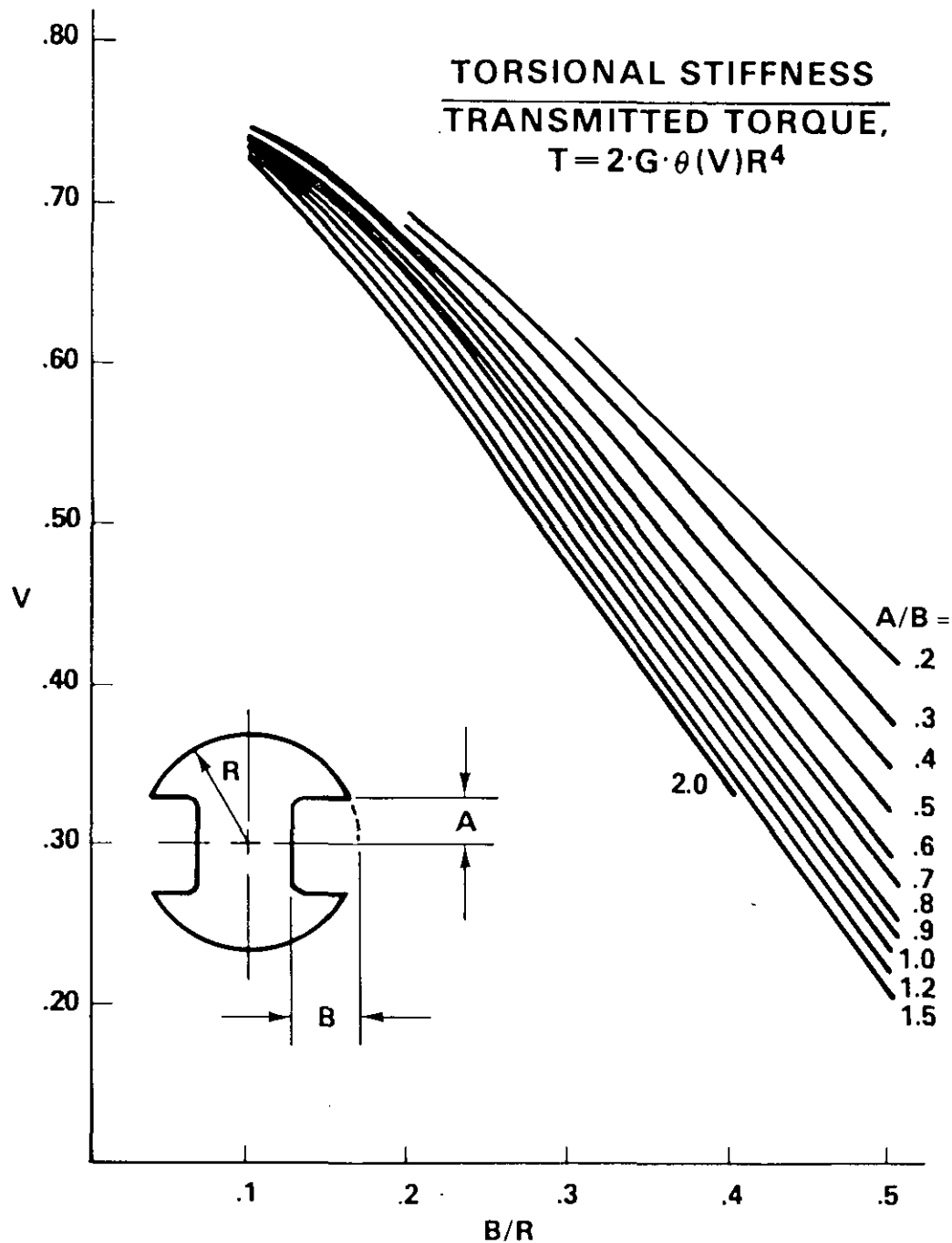
Figure 6. Two keyway shaft, torque.

Table 6. Two keyway shaft, volume factor (V)

A/B	B/R				
	0.1	0.2	0.3	0.4	0.5
0.2			.6187	.5226	.4195
0.3		.6927	.6008	.4944	.3831
0.4		.6853	.5848	.4688	.3517
0.5	.7524	.6753	.5678	.4457	.3246
0.6	.7511	.6698	.5562	.4277	.3014
0.7	.7496	.6625	.5429	.4112	.2818
0.8	.7477	.6558	.5319	.3962	.2655
0.9	.7454	.6505	.5221	.3829	.2522
1.0	.7426	.6433	.5117	.3713	.2416
1.2	.7404	.6344	.4974	.3559	.2276
1.5	.7346	.6215	.4813	.3416	.2197
2.0	.7283	.6086	.4703	.3373	

15
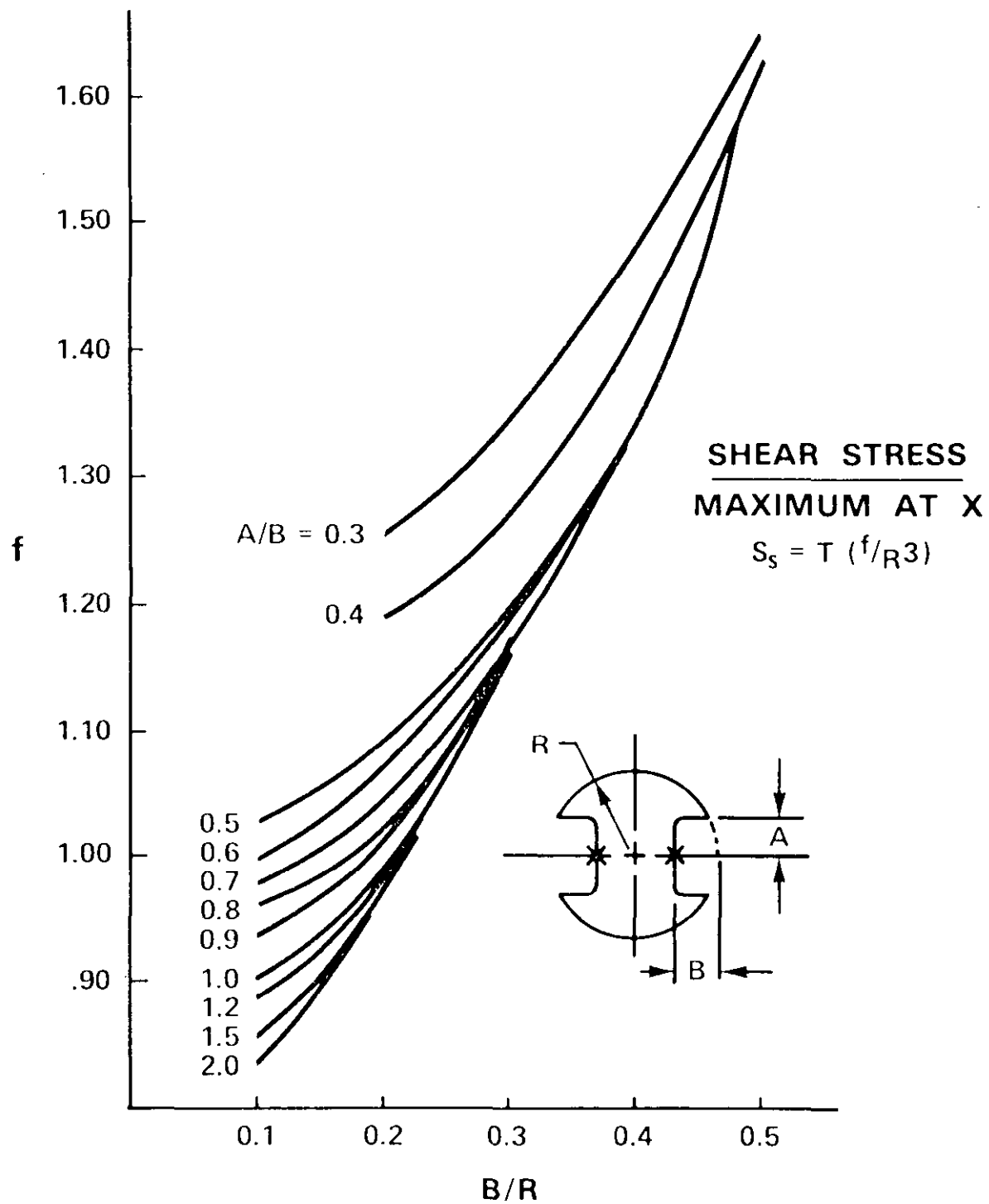
Figure 7. Two keyway shaft, stress.

TORSIONAL STIFFNESS

$$\overline{\text{TRANSMITTED TORQUE,}}$$
$$T = 2 \cdot G \cdot \theta (V) R^4$$

Figure 8. Four keyway shaft, torque.

18

Table 8. Four keyway shaft, volume factor (V)

A/B	B/R				
	0.1	0.2	0.3	0.4	0.5
0.2			.4806	.3361	.2114
0.3		.6088	.4511	.2965	.1705
0.4		.5952	.4253	.2624	.1384
0.5	.7214	.5769	.3983	.2333	.1140
0.6	.7190	.5672	.3805	.2119	.0962
0.7	.7161	.5541	.3605	.1935	.0842
0.8	.7124	.5422	.3444	.1783	
0.9	.7080	.5330	.3304	.1662	
1.0	.7024	.5203	.3160	.1572	
1.2	.6982	.5051	.2974	.1482	
1.5	.6870	.4832	.2787		
2.0	.6748	.4622	.2692		
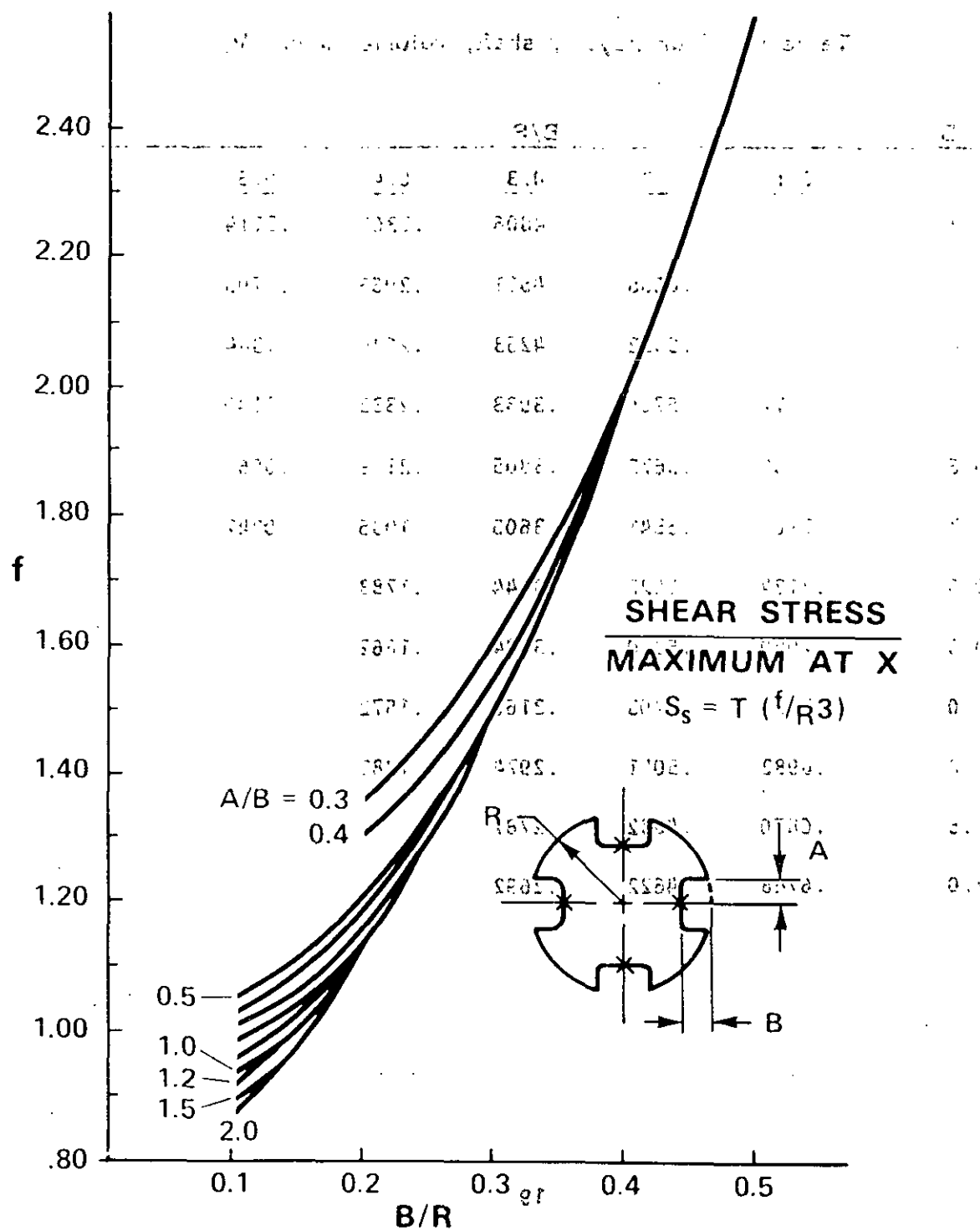
19

Figure 9. Four keyway shaft, stress

Table 9. Four keyway shaft, stress factor (f)

A/B	B/R				
	0.1	0.2	0.3	0.4	0.5
0.2			1.7365	2.1206	2.4931
0.3		1.3566	1.6214	2.0014	2.5784
0.4		1.3011	1.5468	1.9971	2.8271
0.5	1.0371	1.2130	1.5046	2.0591	3.1882
0.6	1.0252	1.1979	1.5115	2.1568	3.6139
0.7	1.0102	1.1737	1.5175	2.2660	4.0368
0.8	.9910	1.1541	1.5382	2.3834	
0.9	.9661	1.1493	1.5609	2.4993	
1.0	.9331	1.1398	1.5899	2.6030	
1.2	.9232	1.1422	1.6424	2.7301	
1.5	.8940	1.1511	1.7092		
2.0	.8796	1.1717	1.7512		
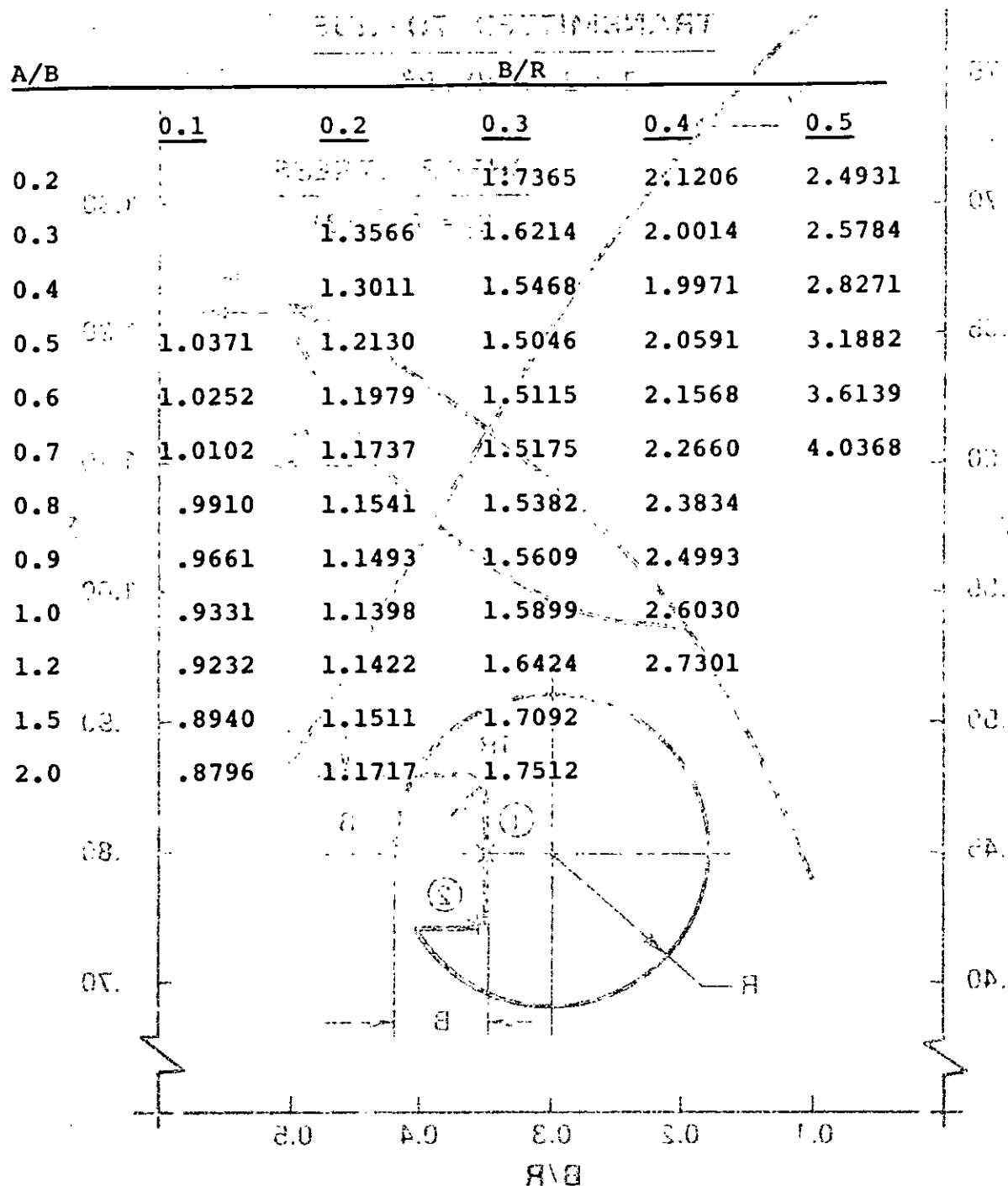
MIL-HDBK-776(AR)
15 September 1981
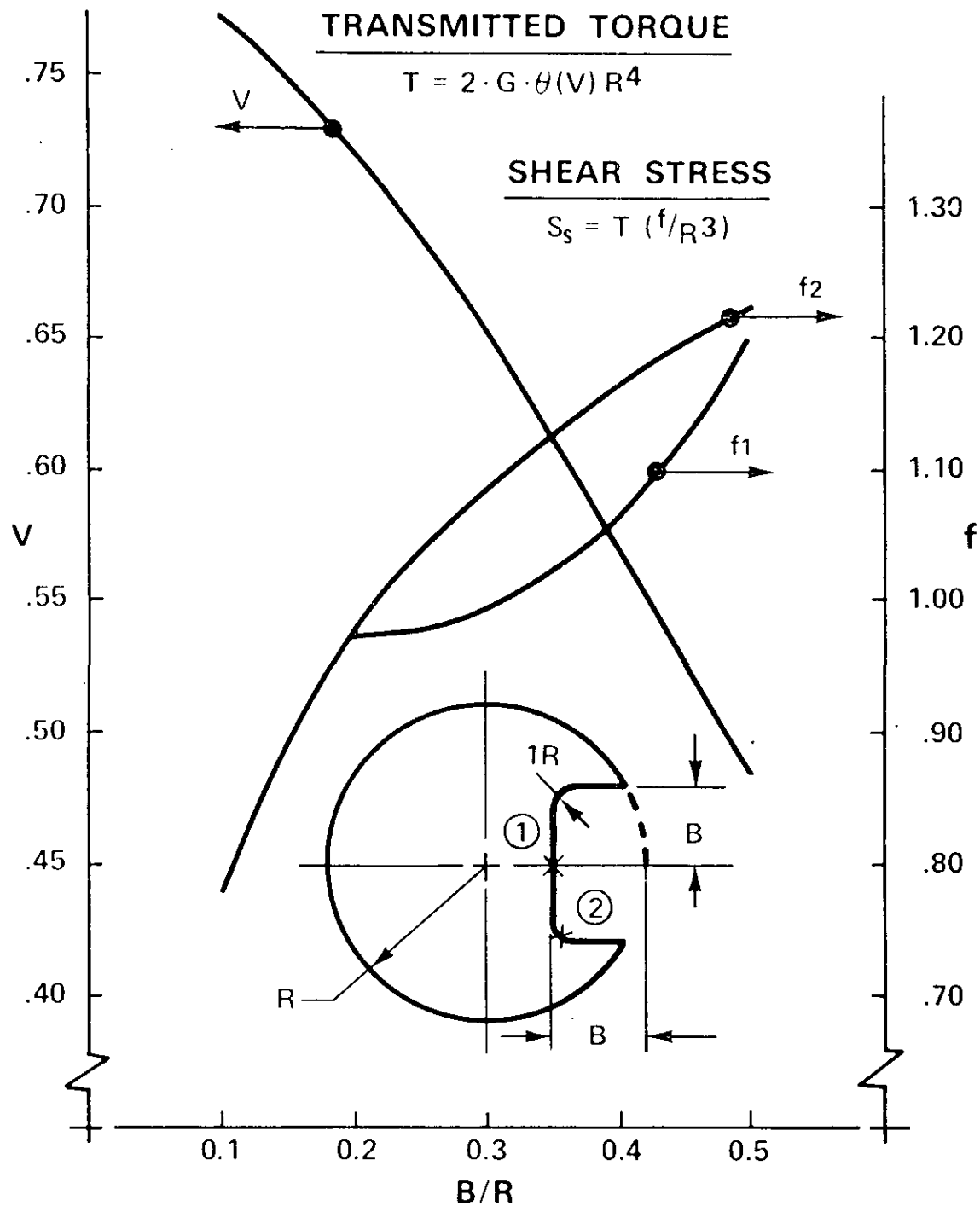
Figure 10.   Single square keyway with inner fillets.

Table 10.   Single square keyway with tight inner fillets

B/R	Volume factor(V)	Stress factor(f)	
		At keyway center(1)	At inner fillet(2)
0.1	.7703		.7804
0.2	.7206	.9715	.9777
0.3	.6504	.9941	1.0817
0.4	.5690	1.0735	1.1641
0.5	.4840	1.1977	1.2245
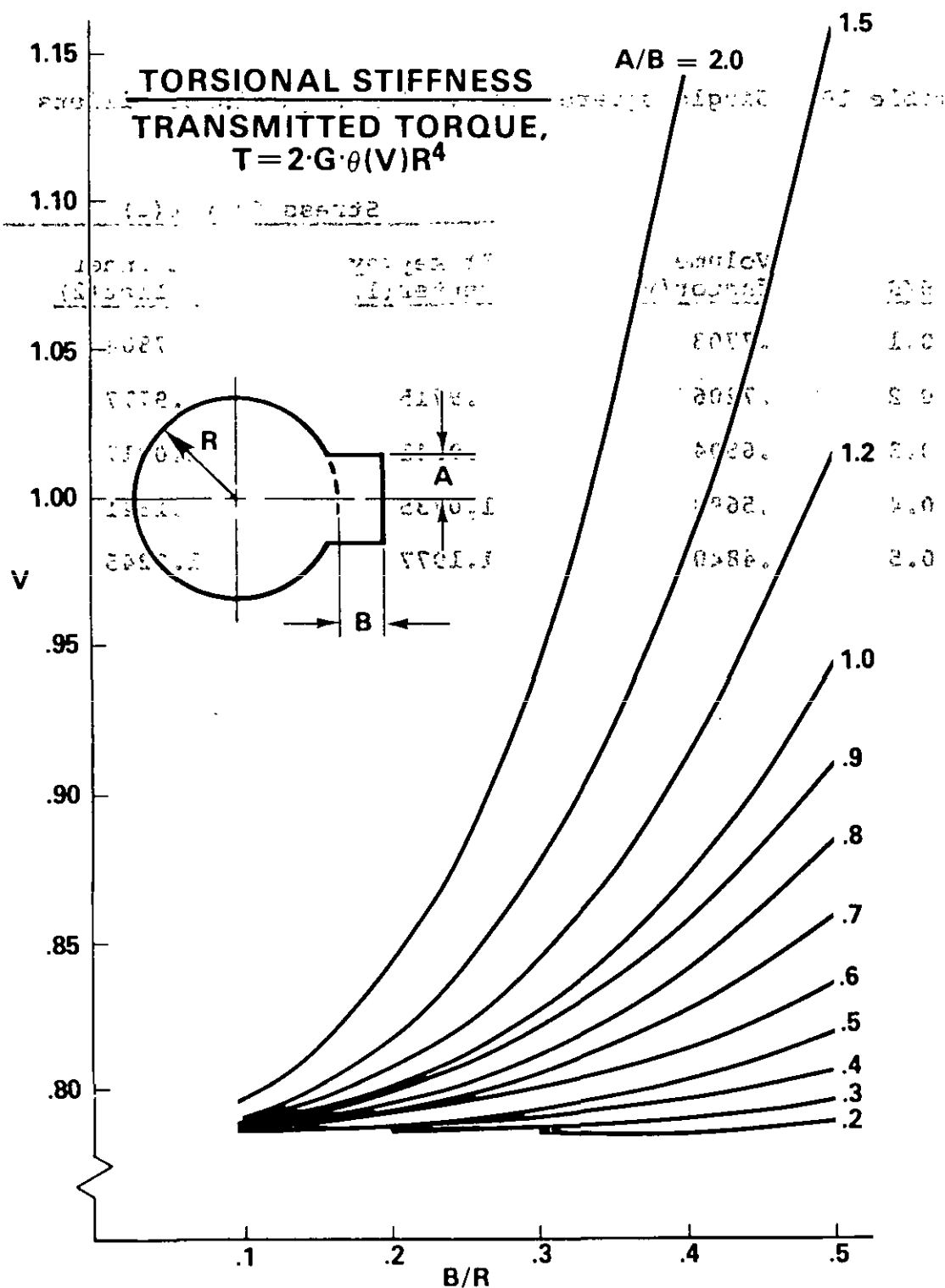
Figure 11.   Single spline shaft, torque.

Table 11. Single spline shaft, volume factor (V)

A/B	B/R				
	0.1	0.2	0.3	0.4	0.5
0.2			.7853	.7865	.7878
0.3		.7853	.7870	.7906	.7944
0.4		.7864	.7903	.7968	.8048
0.5	.7845	.7874	.7933	.8035	.8189
0.6	.7852	.7899	.7993	.8143	.8362
0.7	.7857	.7918	.8059	.8270	.8580
0.8	.7862	.7950	.8113	.8390	.8832
0.9	.7866	.7976	.8202	.8560	.9110
1.0	.7869	.7996	.8253	.8712	.9433
1.2	.7890	.8071	.8456	.9117	1.0158
1.5	.7907	.8174	.8754	.9800	1.1561
2.0	.7953	.8407	.9420	1.1404	

25

SHEAR STRESS

MAXIMUM AT X

$$S_s = T \left(^f/_R3\right)$$

A/B = 0.2
0.4
0.5
0.6
0.7
0.8
0.9
1.0
1.2
1.5

A/B = 2.0

f

0.65
0.60
0.55
0.50
0.45
0.40

R

A

B

0.1   0.2   0.3   0.4   0.5

B/R
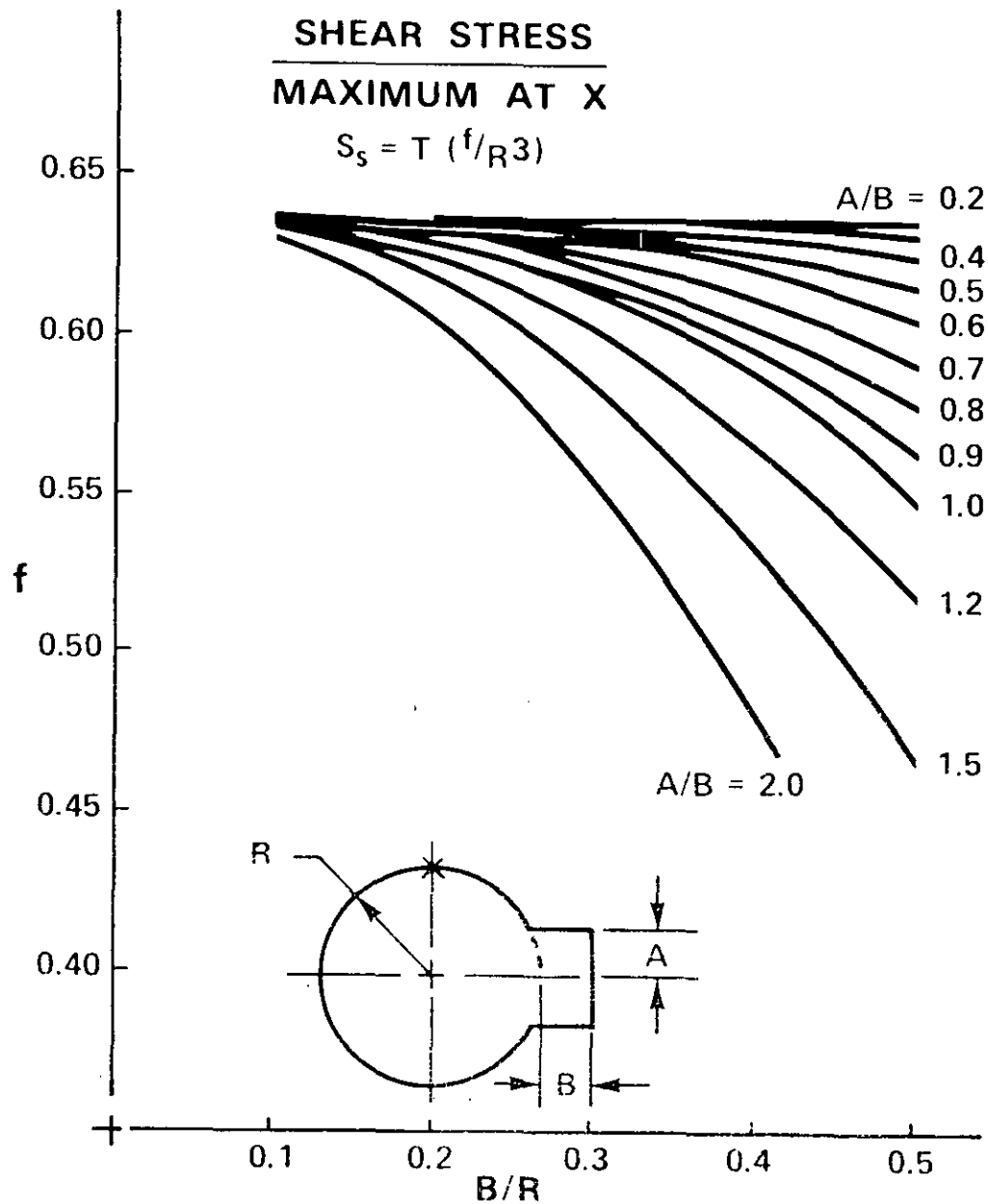
Figure 12. Single spline shaft, stress.

Table 12. Single spline shaft, stress factor (f)

A/B	B/R				
	0.1	0.2	0.3	0.4	0.5
0.2			.6369	.6361	.6352
0.3		.6369	.6358	.6335	.6309
0.4		.6362	.6337	.6295	.6241
0.5	.6374	.6356	.6317	.6251	.6152
0.6	.6370	.6340	.6280	.6184	.6047
0.7	.6366	.6328	.6239	.6107	.5920
0.8	.6364	.6308	.6205	.6035	.5781
0.9	.6361	.6291	.6152	.5939	.5638
1.0	.6359	.6279	.6120	.5854	.5483
1.2	.6346	.6233	.6004	.5648	.5173
1.5	.6335	.6172	.5842	.5340	.4704
2.0	.6307	.6038	.5525	.4798	.4331
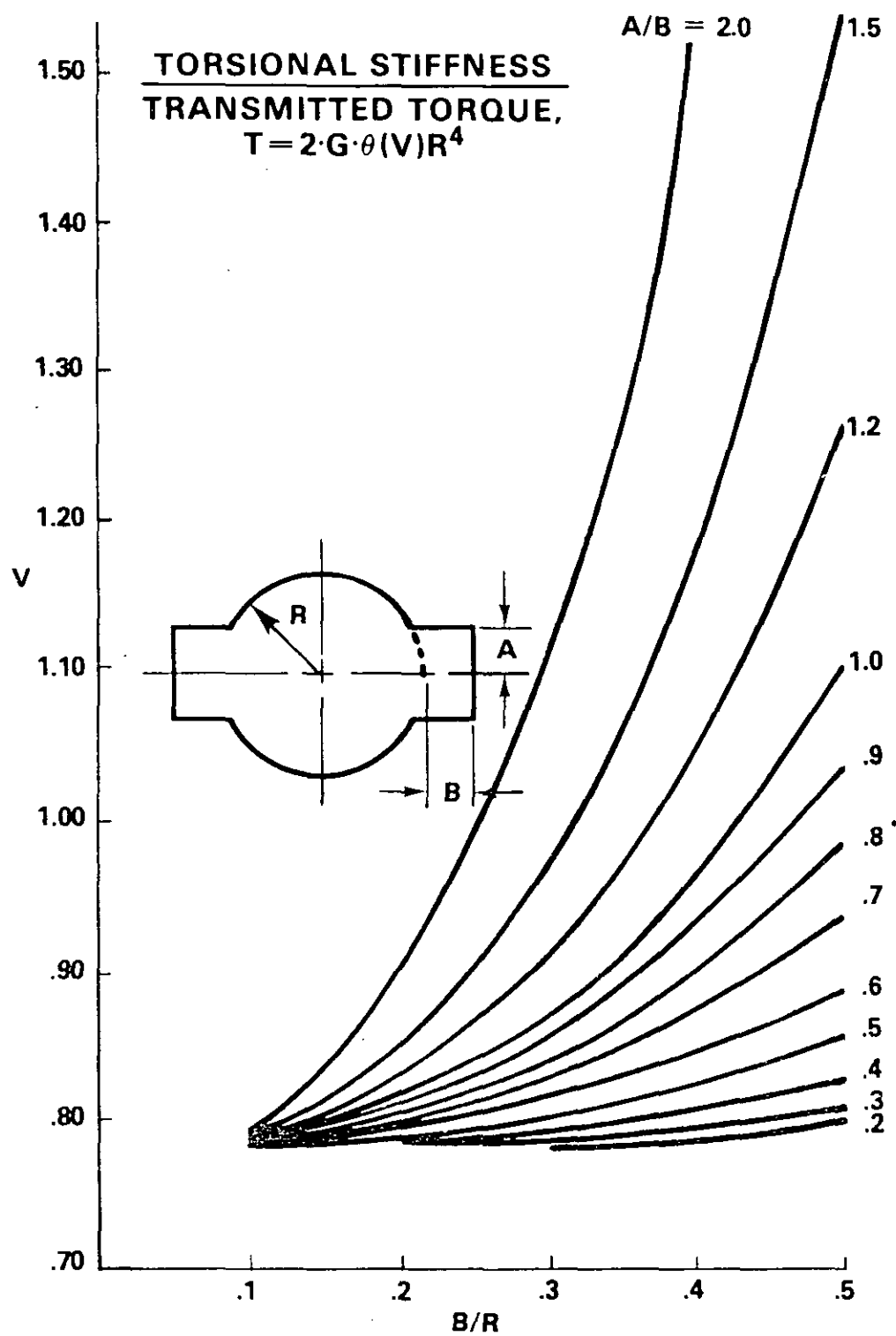
Figure 13. Two spline shaft, torque.

Table 13. Two spline shaft, volume factor (V)

A/B	B/R				
	0.1	0.2	0.3	0.4	0.5
0.2			.7865	.7889	.7914
0.3		.7864	.7899	.7970	.8047
0.4		.7886	.7965	.8095	.8255
0.5	.7850	.7906	.8026	.8229	.8538
0.6	.7863	.7958	.8145	.8446	.8886
0.7	.7874	.7994	.8278	.8701	.9326
0.8	.7883	.8059	.8386	.8945	.9837
0.9	.7891	.8111	.8565	.9288	1.0400
1.0	.7897	.8152	.8668	.9595	1.1058
1.2	.7940	.8302	.9078	1.0418	1.2547
1.5	.7973	.8509	.9682	1.1818	1.5471
2.0	.8066	.8980	1.1045	1.5172	

29

SHEAR STRESS

MAXIMUM AT X

$$S_s = T \left(f/R^3 \right)$$
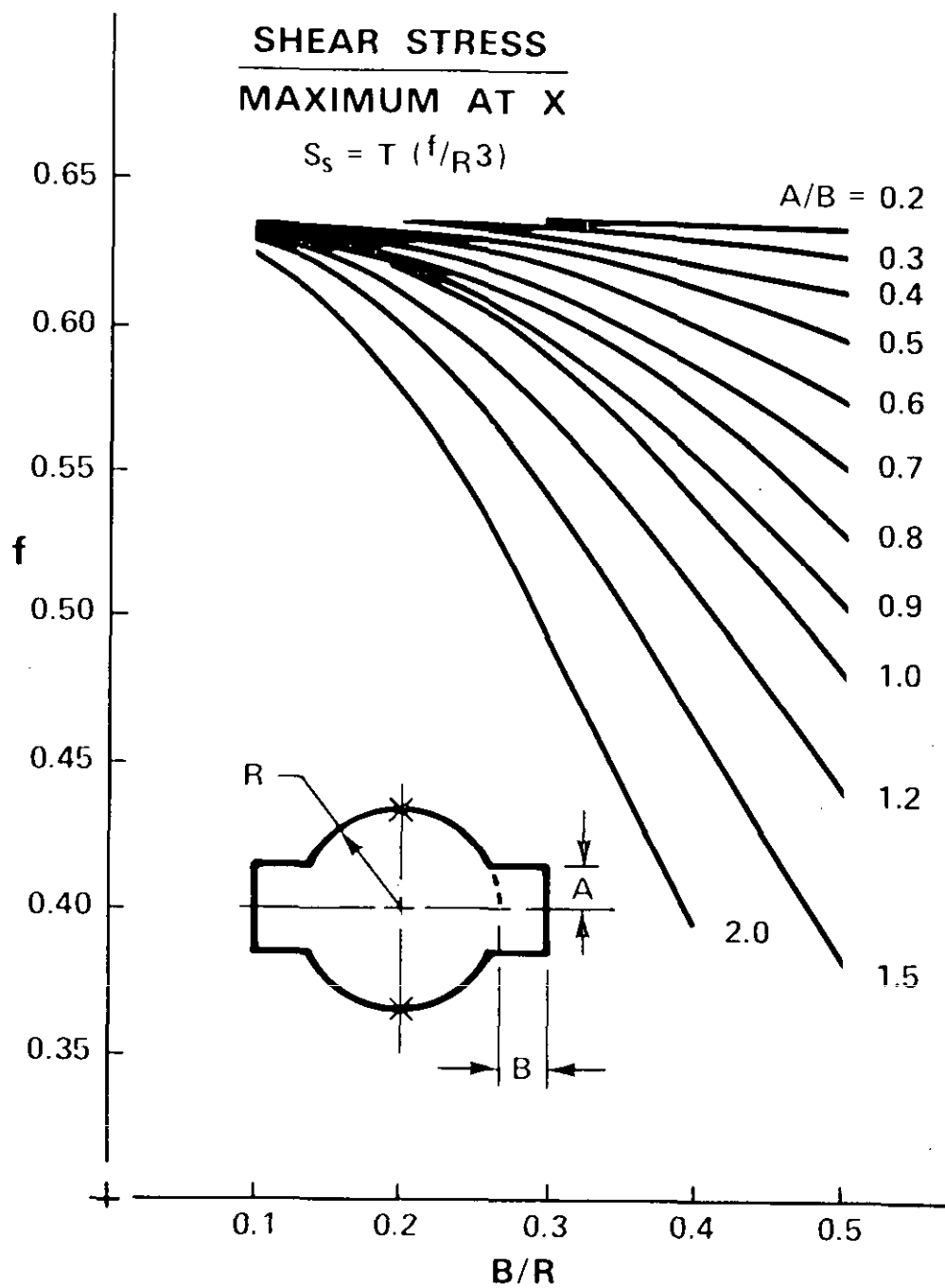
Figure 14. Two spline shaft, stress.

Table 14.   Two spline shaft, stress factor (f)

A/B	B/R				
	0.1	0.2	0.3	0.4	0.5
0.2			.6362	.6346	.6329
0.3		.6362	.6340	.6294	.6243
0.4		.6348	.6298	.6215	.6113
0.5	.6371	.6336	.6259	.6131	.5946
0.6	.6363	.6303	.6187	.6004	.5753
0.7	.6357	.6281	.6108	.5862	.5532
0.8	.6351	.6241	.6043	.5732	.5300
0.9	.6346	.6209	.5944	.5564	.5071
1.0	.6342	.6184	.5887	.5421	.4836
1.2	.6315	.6097	.5678	.5088	.4398
1.5	.6295	.5981	.5402	.4632	.3815
2.0	.6240	.5740	.4903	.3937	
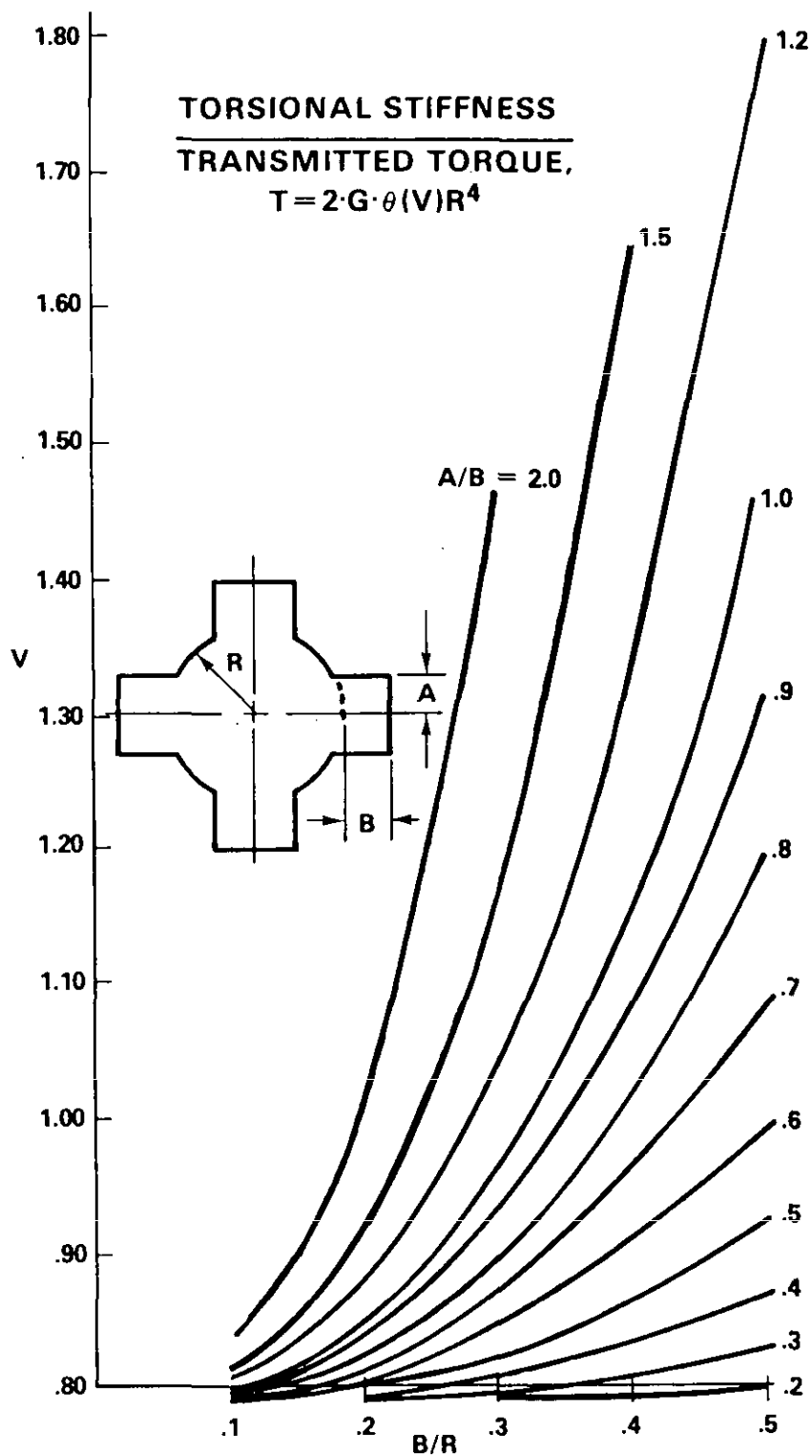
Figure 15. Four spline shaft, torque.

Table 15.   Four spline shaft, volume factor (V)

A/B	B/R				
	0.1	0.2	0.3	0.4	0.5
0.2			.7888	.7937	.7989
0.3		.7887	.7957	.8101	.8254
0.4		.7932	.8090	.8352	.8674
0.5	.7859	.7971	.8213	.8623	.9250
0.6	.7885	.8076	.8452	.9063	.9962
0.7	.7906	.8149	.8723	.9588	1.0877
0.8	.7924	.8280	.8944	1.0090	1.1950
0.9	.7940	.8386	.9310	1.0808	1.3158
1.0	.7954	.8467	.9519	1.1455	1.4601
1.2	.8040	.8773	1.0378	1.3239	1.8021
1.5	.8106	.9196	1.1663	1.6438	
2.0	.8292	1.0180	1.4739		

33

SHEAR STRESS
MAXIMUM AT X

$$S_s = T \left(f/_R3 \right)$$
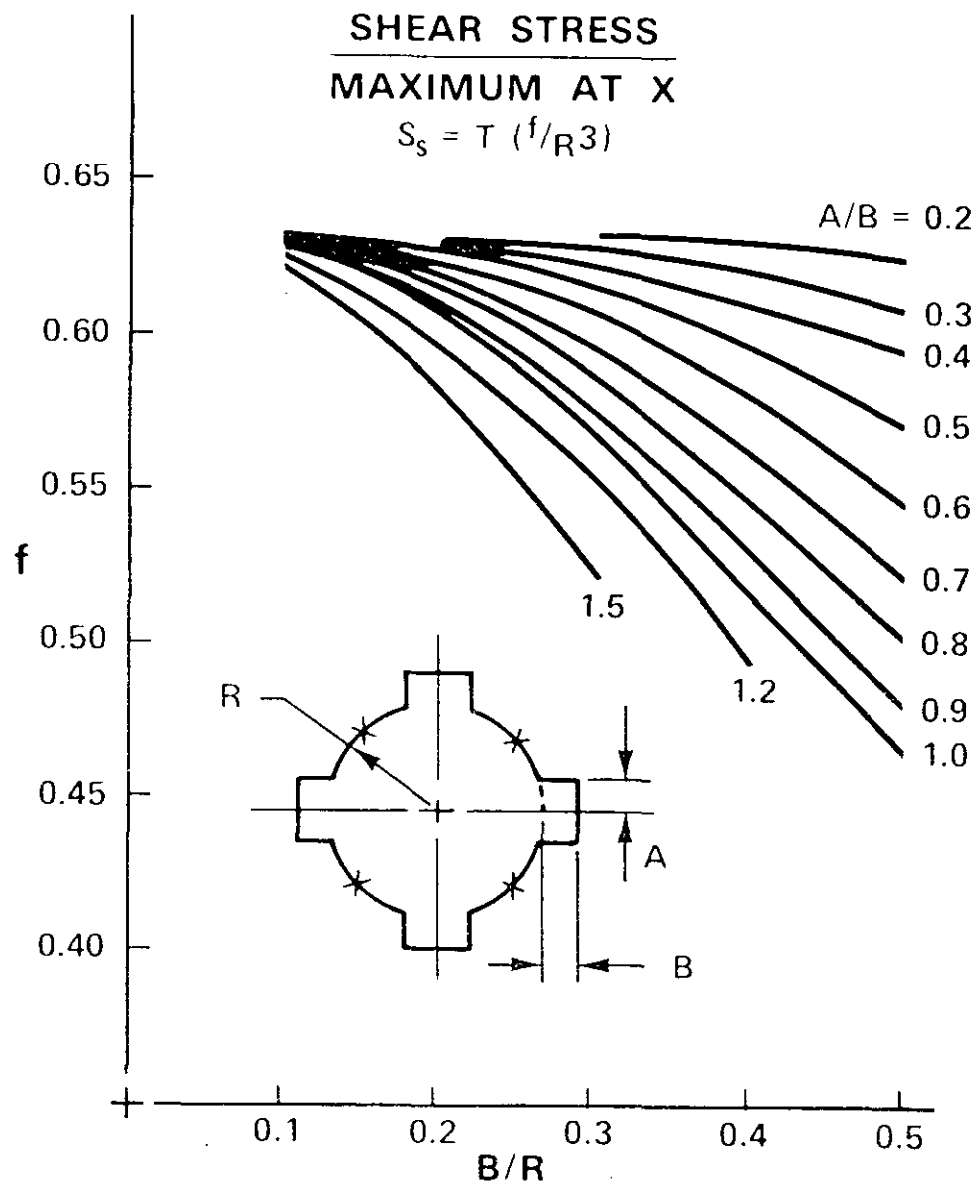
Figure 16. Four spline shaft, stress

Table 16.   Four spline shaft, stress factor (f)

A/B	B/R				
	0.1	0.2	0.3	0.4	0.5
0.2			.6356	.6332	.6305
0.3		.6356	.6323	.6256	.6176
0.4		.6336	.6263	.6142	.5986
0.5	.6369	.6318	.6206	.6019	.5756
0.6	.6358	.6273	.6106	.5848	.5510
0.7	.6349	.6240	.6001	.5670	.5257
0.8	.6341	.6187	.5913	.5516	.5028
0.9	.6334	.6144	.5794	.5344	.4842
1.0	.6328	.6109	.5720	.5199	.4714
1.2	.6293	.5998	.5508	.4989	
1.5	.6265	.5860	.5279		
2.0	.6192	.5630			

35

TORSIONAL STIFFNESS OF SQUARE KEYWAYS & SPLINES

1 KEYWAY

2

4

V

B/R

TRANSMITTED TORQUE,

$$T = 2 \cdot G \cdot \theta (V) R^4$$

4

2

1 LOBE

V

B/R

36
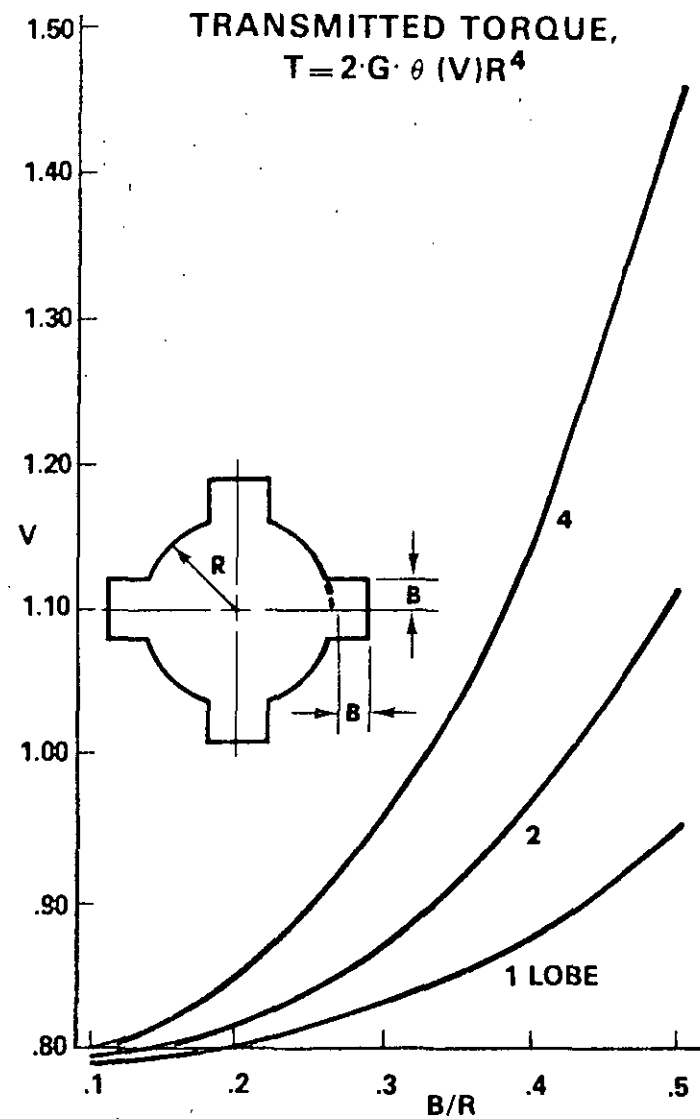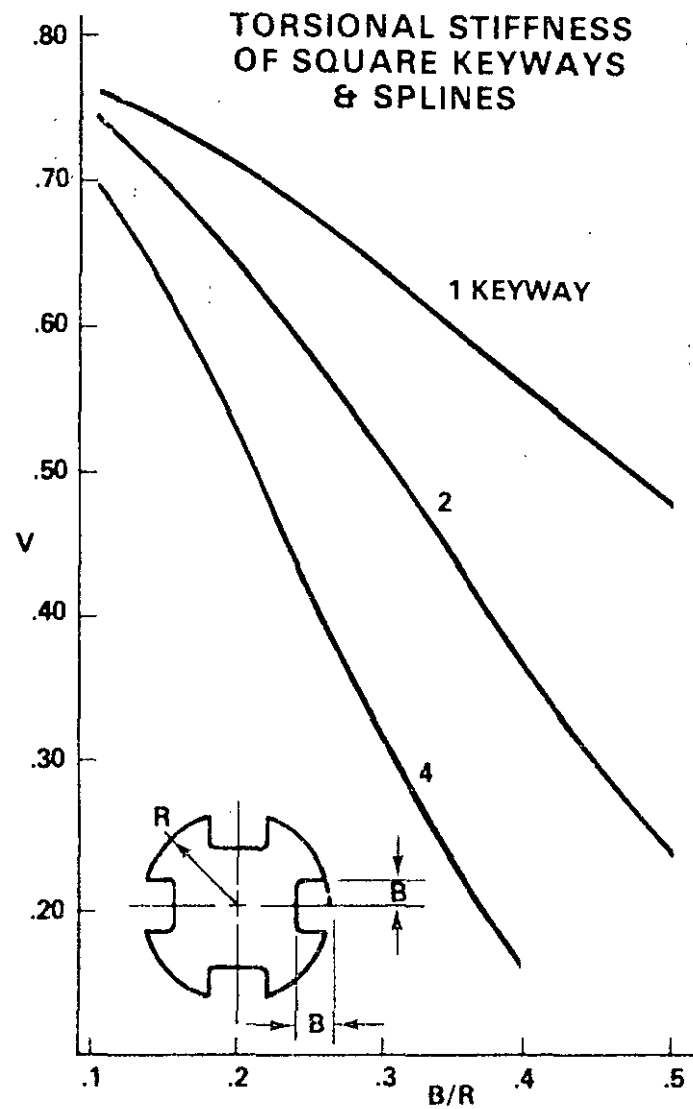
Figure 17. Square keyways and external splines, torque.

Table 17.   Square keyways and external splines, volume factor (V)

B/R	One keyway	Two keyways	Four keyways
0.1	.7633	.7426	.7024
0.2	.7125	.6433	.5203
0.3	.6424	.5117	.3160
0.4	.5619	.3713	.1572
0.5	.4783	.2416	

B/R	One spline	Two splines	Four splines
0.1	.7869	.7897	.7954
0.2	.7996	.8152	.8467
0.3	.8253	.8668	.9519
0.4	.8712	.9595	1.1455
0.5	.9433	1.1058	1.4601

37

SHEAR STRESS
MAXIMUM AT X
$S_S = T\,(^f/_R3)$
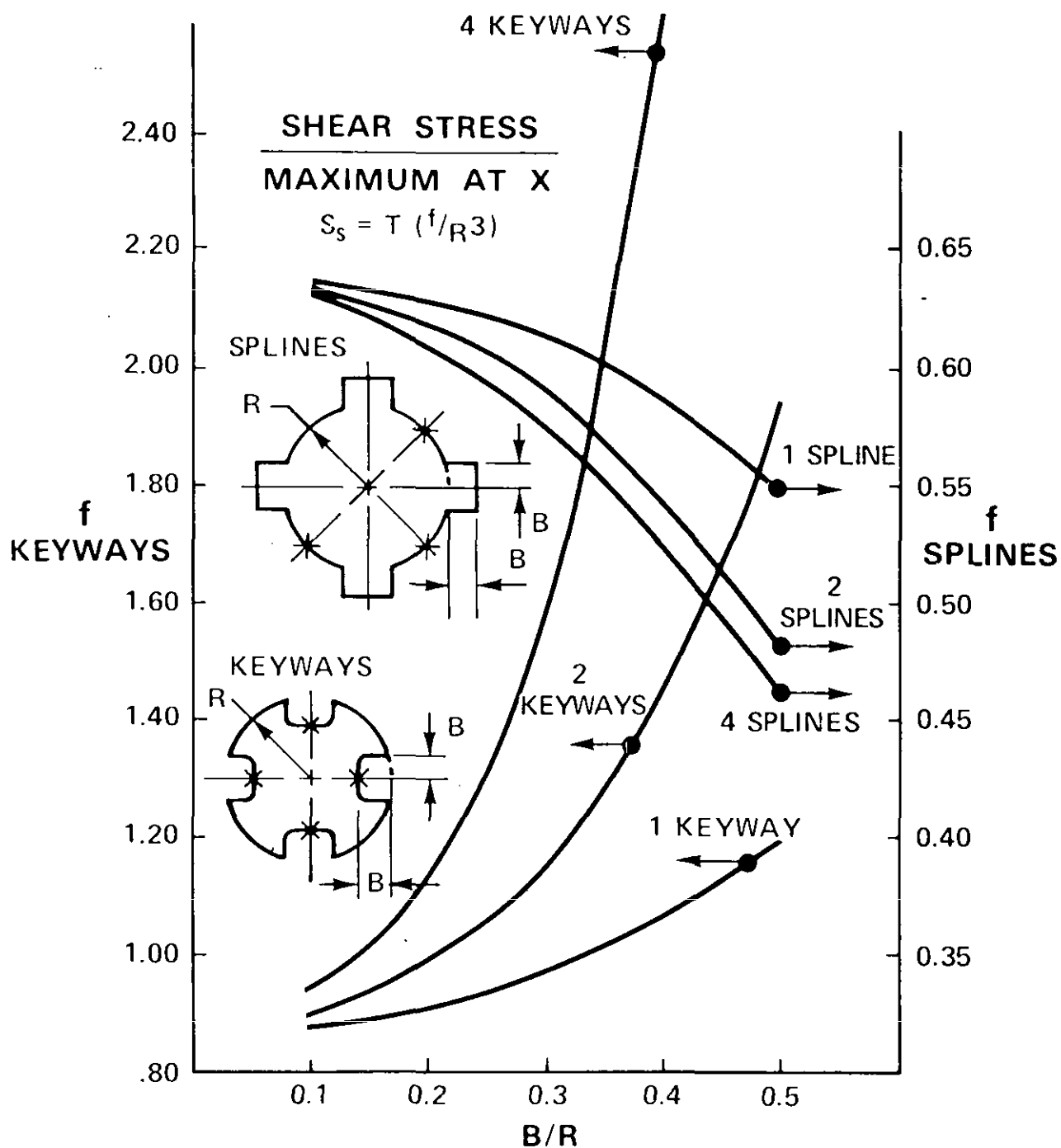
Figure 18. Square keyways and external splines, stress.

Table 18. Square keyways & external splines, stress factor(f)

B/R	One keyway	Two keyways	Four keyways
0.1	.8773	.8978	.9331
0.2	.9131	.9916	1.1398
0.3	.9749	1.1625	1.5899
0.4	1.0691	1.4532	2.6030
0.5	1.2009	1.9502	

B/R	One spline	Two splines	Four splines
0.1	.6359	.6342	.6328
0.2	.6279	.6184	.6109
0.3	.6120	.5887	.5720
0.4	.5854	.5421	.5199
0.5	.5483	.4836	.4714

39
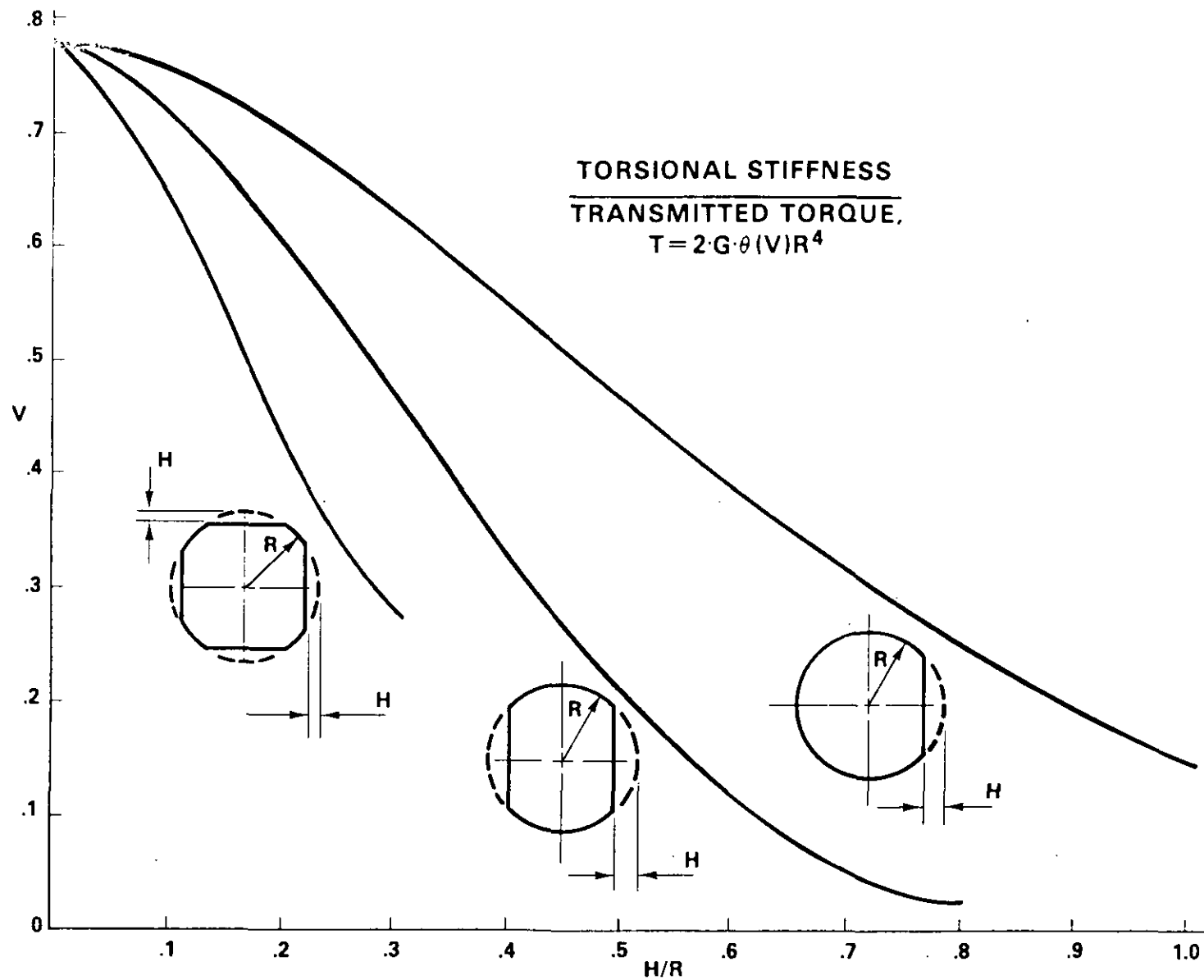
Figure 19. Milled shaft, torque.

Table 19. Milled shaft, volume factor (V)

H/R	One flat	Two flats	Four flats
0	.7813	.7811	.7811
0.1	.7617	.7149	.6520
0.2	.7018	.5998	.450l
0.29289			.2777
0.3	.6291	.4667	
0.4	.5510	.3349	
0.5	.4717	.2168	
0.6	.3951	.1225	
0.7	.3228	.0559	
0.8	.2568	.0173	
0.9	.1980		
1.0	.1460		

41

SHEAR STRESS
MAXIMUM AT CENTER OF FLATS, AT X

$$S_s = T \left(f/R^3\right)$$
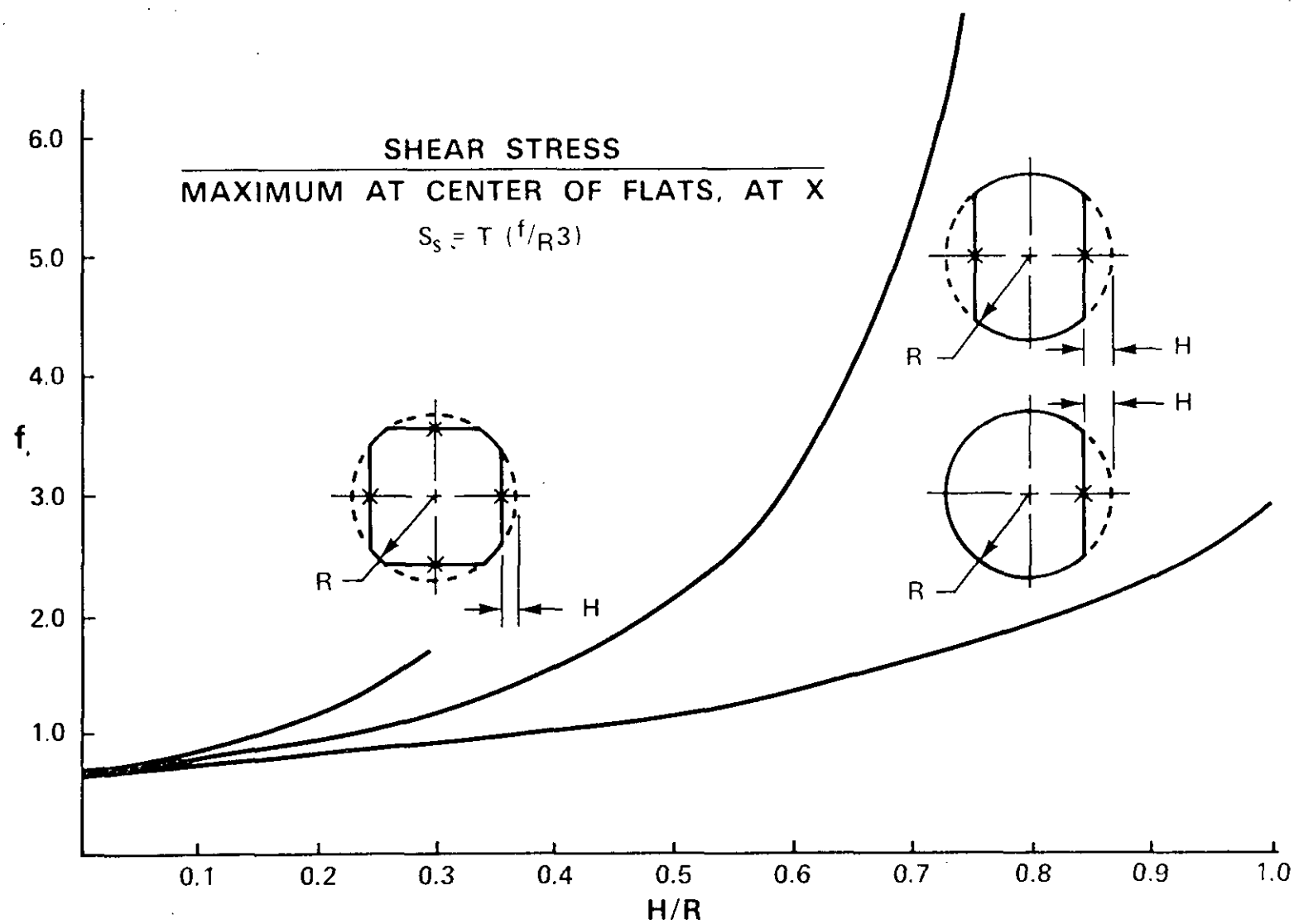
Figure 20. Milled shaft, stress.

Table 20.   Milled shaft, stress factor (f)

H/R	One flat	Two flats	Four flats
0.1	.7749	.8199	.8743
0.2	.8571	.9776	1.1848
0.29289			1.7004
0.3	.9485	1.2045	
0.4	1.0593	1.5520	
0.5	1.1977	2.1237	
0.6	1.3725	3.1455	
0.7	1.5987	5.3129	
0.8	1.8975	11.5433	
0.9	2.3049		
1.0	2.8935		

43

TORSIONAL STIFFNESS

TRANSMITTED TORQUE

$$T = 2 \cdot G \cdot \theta \, (V) A^4$$

SHEAR STRESS

(MAXIMUM AT MID-POINT OF LONG EDGE)

$$S_s = T \, (f/_A 3)$$

Figure 21. Rectangular shaft.

44
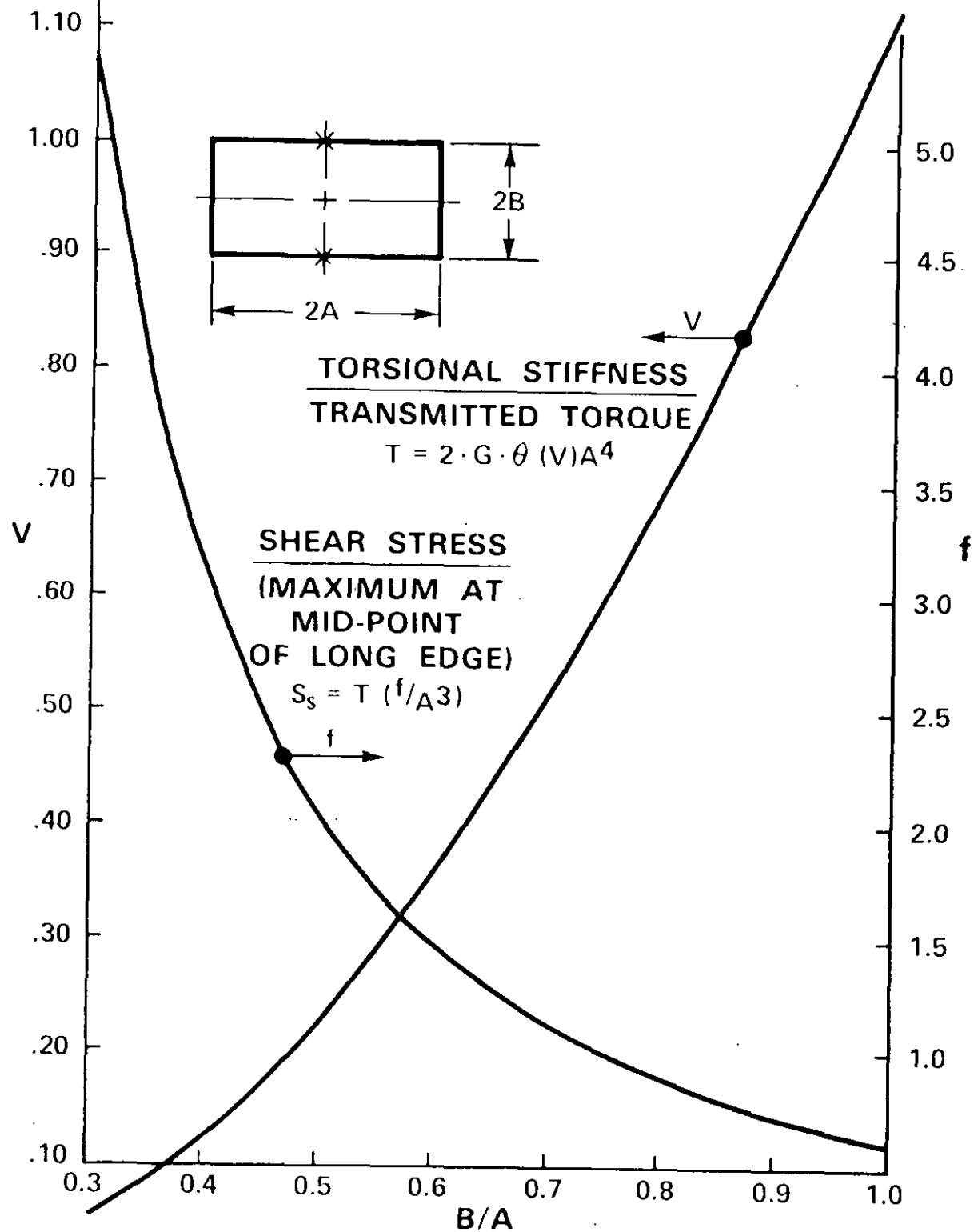
Table 21.   Rectangular shaft

B/A	Volume factor(V)	Stress factor(f)
0.3	.05635	5.2697
0.4	.1248	3.0928
0.5	.2250	2.0587
0.6	.3559	1.4805
0.7	.5146	1.1230
0.8	.6971	.8862
0.9	.8991	.7212
1.0	1.1167	.6015

**TORSIONAL
STIFFNESS
TRANSMITTED TORQUE,**

$$T = 2 \cdot G \cdot \theta (V) R^4$$
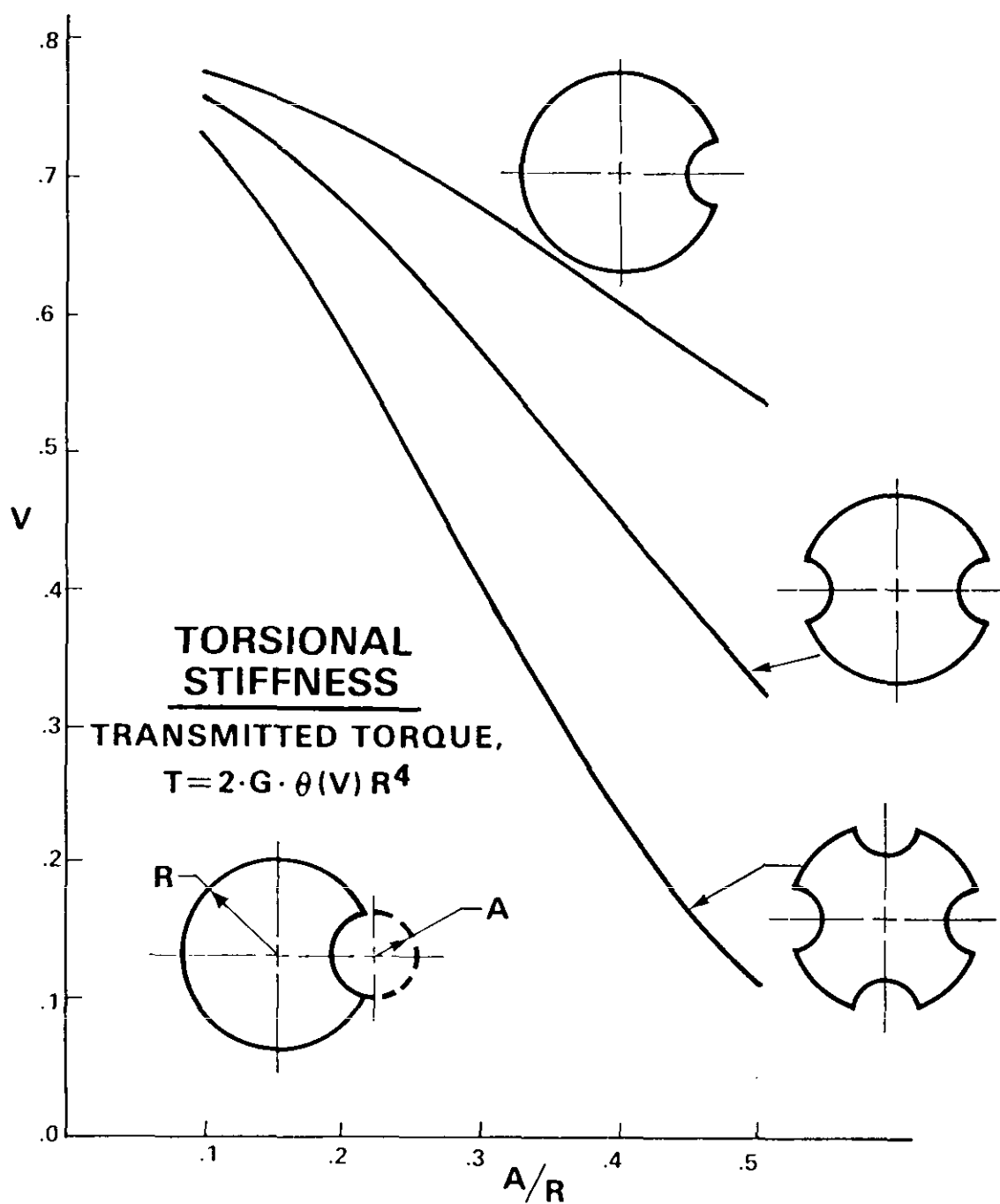
Figure 22. Pinned shaft, torque.

.46

Table 22. Pinned shaft, volume factor (V)

A/R	One groove	Two grooves	Four grooves
0.1	.7700	.7558	.7280
0.2	.7316	.6803	.5855
0.3	.6760	.5738	.4062
0.4	.6087	.4521	.2374
0.5	.5349	.3300	.1118

47
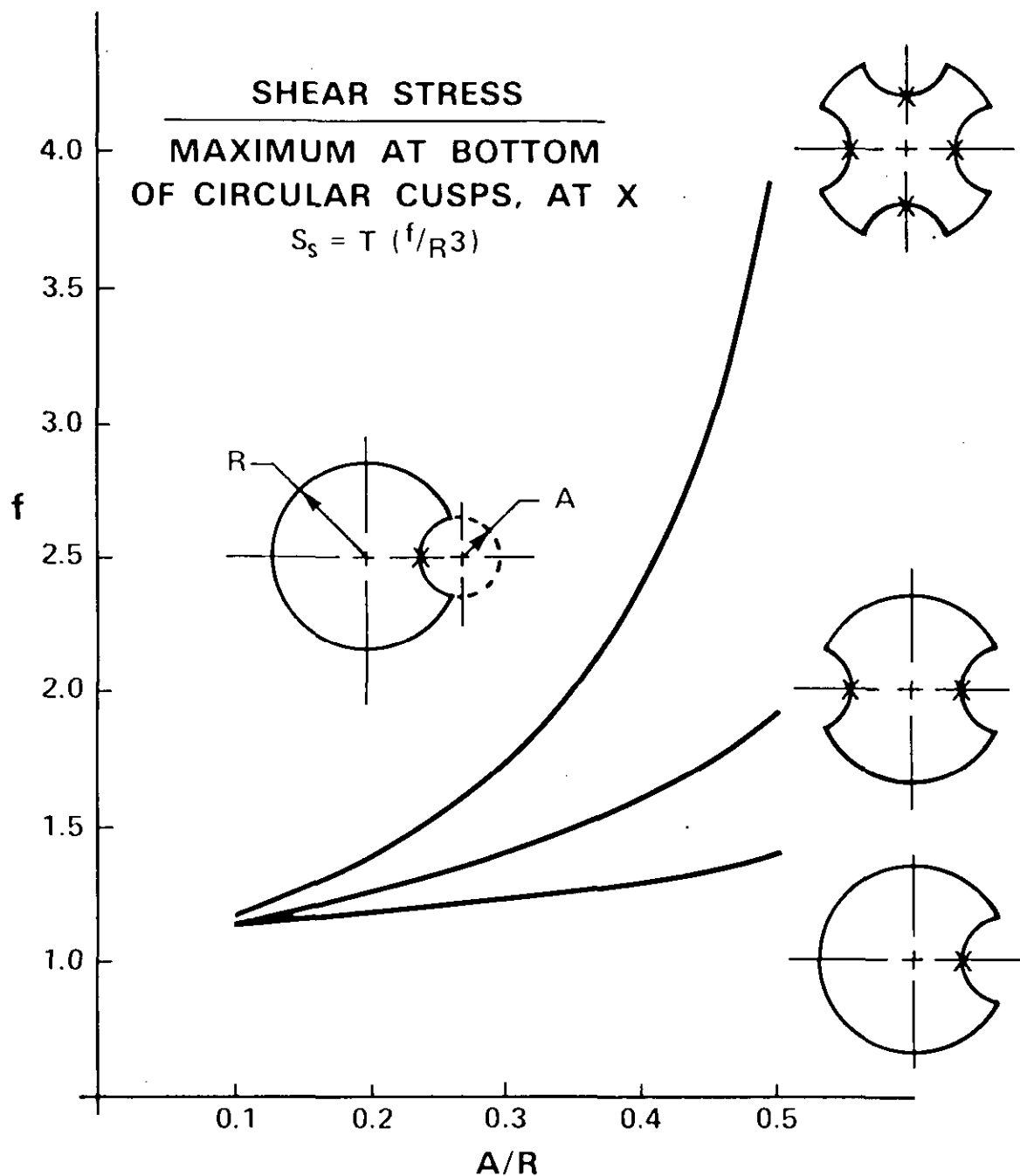
Figure 23. Pinned shaft, stress.

Table 23.   Pinned shaft, stress factor(f)

A/R	One groove	Two grooves	Four grooves
0.1	1.1197	1.1374	1.1674
0.2	1.1804	1.2520	1.3800
0.3	1.2286	1.3939	1.7281
0.4	1.2894	1.6015	2.3912
0.5	1.3822	1.9211	3.8744

TORSIONAL STIFFNESS

TRANSMITTED TORQUE, $T = 2 \cdot G \cdot \theta (V) S^4$

Figure 24. Cross shaft, torque.

50
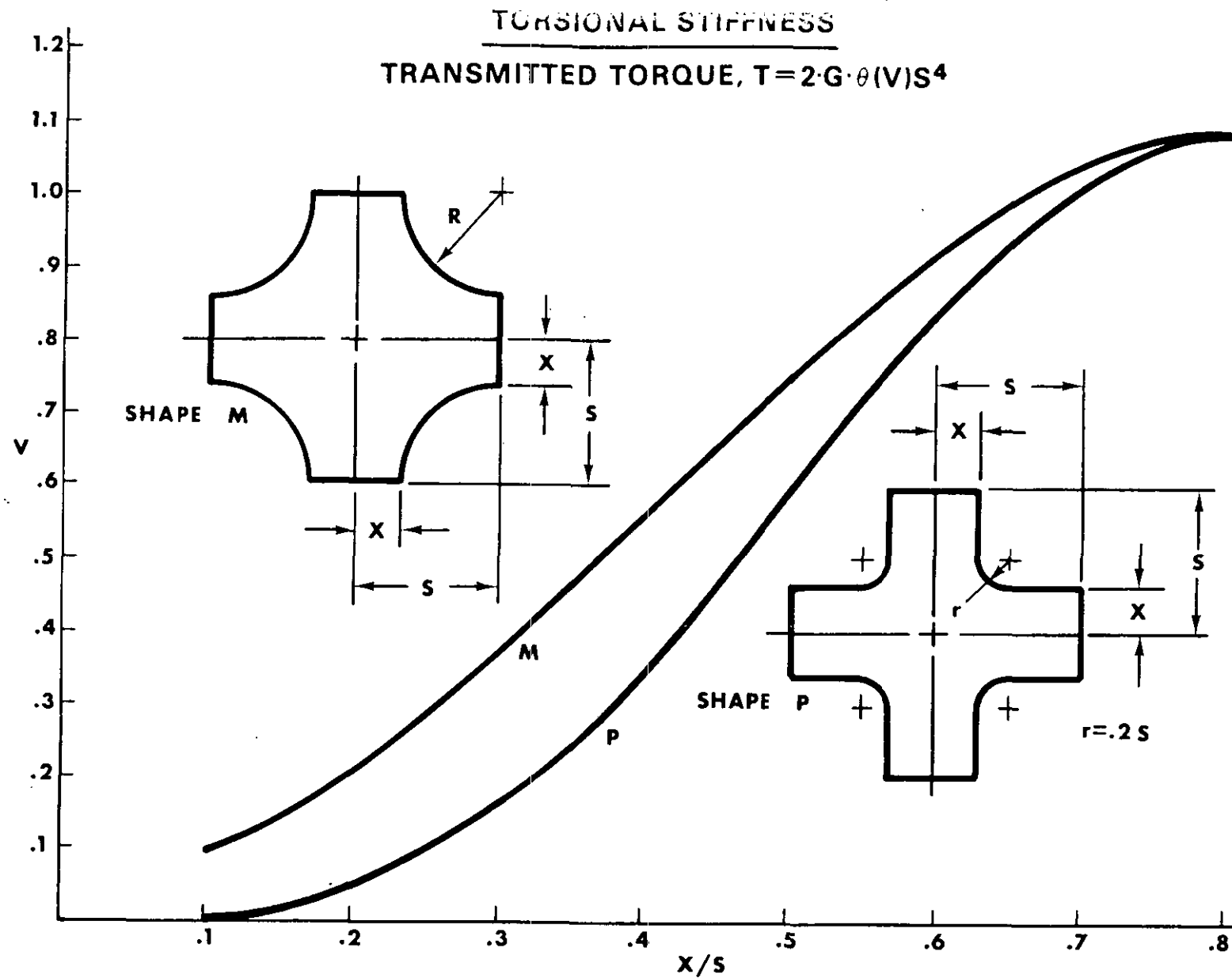
Table 24. Cross shaft, volume factor (V)

X/S	Shape P	Shape M
0.1	.00741	.09907
0.2	.05219	.2120
0.3	.1642	.3767
0.4	.3538	.5714
0.5	.5947	.7639
0.6	.8302	.9247
0.7	1.0058	1.0368
0.8	1.0981	1.0981

SHEAR STRESS

MAXIMUMS AT a & b

$$S_s = T \left({}^f/_S 3 \right)$$
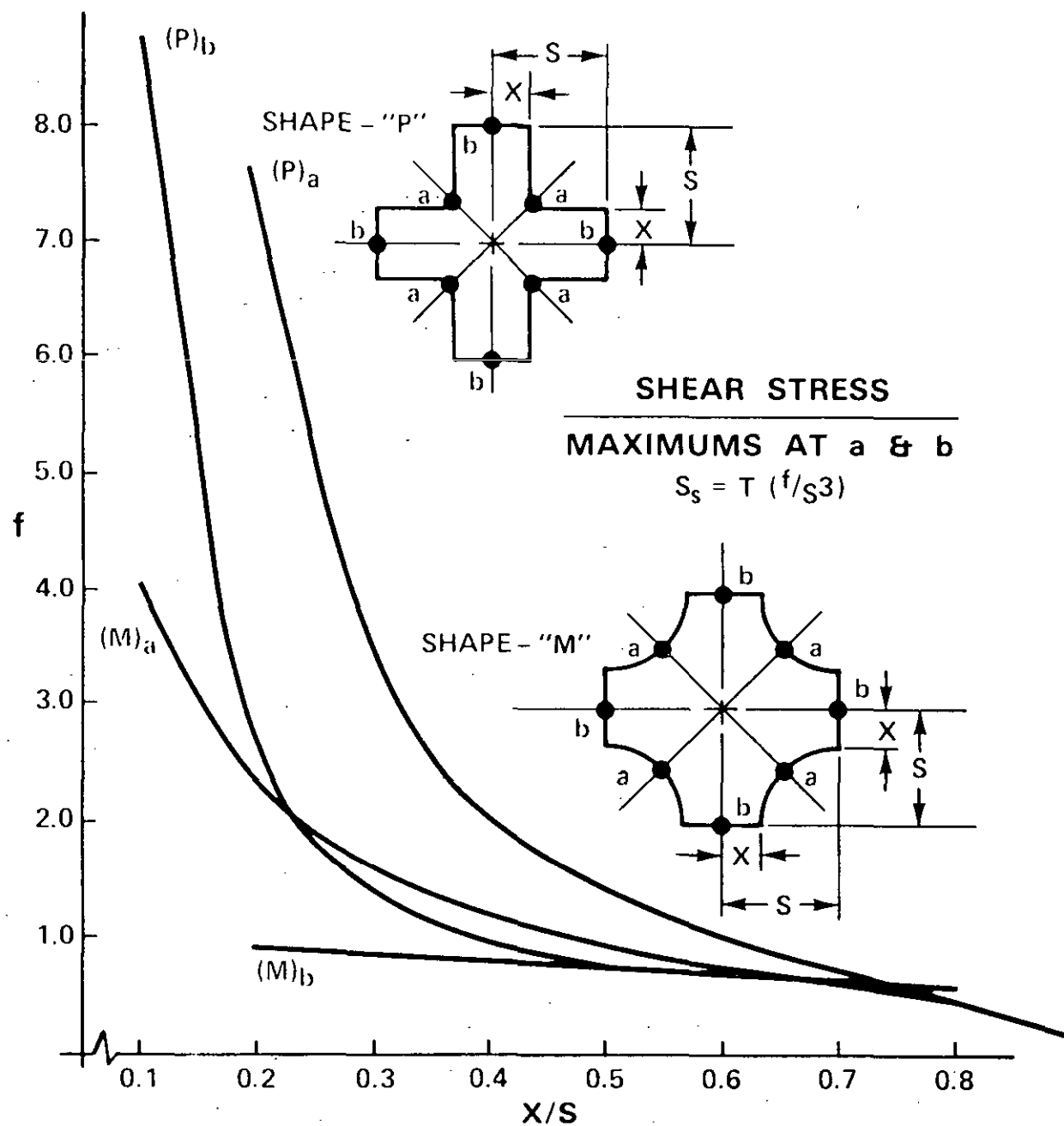
Figure 25. Cross shaft, stress

Table 25. Cross shaft, stress factor(f)

X/S	Shape P		Shape M	
	At a	At b	At a	At b
0.1	26.8826	8.7805	4.0676	.7564
0.2	7.2946	2.7669	2.3702	.9225
0.3	3.5252	1.4172	1.5818	.8651
0.4	2.1192	.9709	1.1844	.7806
0.5		.7849	.9210	.7109
0.6		.6903	.7576	.6606
0.7		.6366	.6059	.6275
0.8		.6090	.4763	.6090

53

MIL-HDBK-776(AR)
15 September 1981

ACCURACY OF THE COMPUTERIZED SOLUTION

To compare the SHAFT (computer) analysis of the torsion of a solid circular shaft with the exact, classical textbook solution, one quadrant of a unit-radius shaft was run with two finite-different grid spacings and the results of the equations were compared, as follows:

Equation Comparison		SHAFT		Exact
Torque		$2G\theta(V)R^4$	⟷	$G\theta J$
		$2(V)R^4$	⟷	J
		$2(V)R^4$	⟷	$(\pi/2)R^4$
		$2V$	⟷	$(\pi/2)$
Shear stress (max)		$G\theta(\frac{d\phi}{ds})R$	⟷	$G\theta R$
		$(\frac{d\phi}{ds})$	⟷	$1.$

		SHAFT	Exact	Deviation (%)
Torque	(h=0.125	1.5546	1.5708	1.03
	(h=0.0625)	1.5669	1.5708	0.25
Shear stress.	(h=0.125)	1.0000	1.0	0.
	(h=0.0625)	1.0000	1.0	0.
Area*	(h=0.125)	3.13316	3.14159	0.268
	(h=0.0625)	3.13984	3.14159	0.056

*Used for internal program checking.

The mathematical model used in the SHAFT computer program generation of this handbook is described in appendix A.

54

PARALLEL SHAFT CONCEPT

The torsional rigidity of a uniform circular shaft, i.e., the torque required to produce unit (one radian) displacement, is:

$$C = T/\theta = G \cdot J$$

In the terminology of the membrane analogy, the torsional rigidity of non-circular shafts is defined as:

$$C = T/\theta = 2 \cdot G \cdot \theta(V) f(R)/\theta$$

The overall torsional rigidity of a system consisting of a number of shafts in parallel (fig. 26) is simply the sum of the torsional rigidities of the individual component shafts.

$$\sum_{i=1}^{N} C_i = C_1 + C_2 + C_3 + \cdots + C_N$$

$$\sum_{i=1}^{N} T_i \theta_i = \theta \sum_{i=1}^{N} T_i = \theta(T_1 + T_2 + T_3 + \cdots + T_N)$$

The torsional rigidity of hollow shafts can be determined by regarding the configuration as a parallel shaft arrangement. The overall torsional rigidity can be obtained by subtracting the torsional rigidity of a shaft having the dimensions of the bore (or inner contour) from that of a shaft having the dimensions of the outer contour. The advantages of being able to apply the principles of superposition (fig. 27-31) to combinations of concentric (inner and outer) shaft contours are obvious. If, for example, design charts have been prepared for 20 different shaft shapes, then 400 different solutions to all possible combinations of inner and outer shaft contours (20 inner x 20 outer) are available.

55

PARALLEL SHAFTS

MEMBRANE ANALOGY
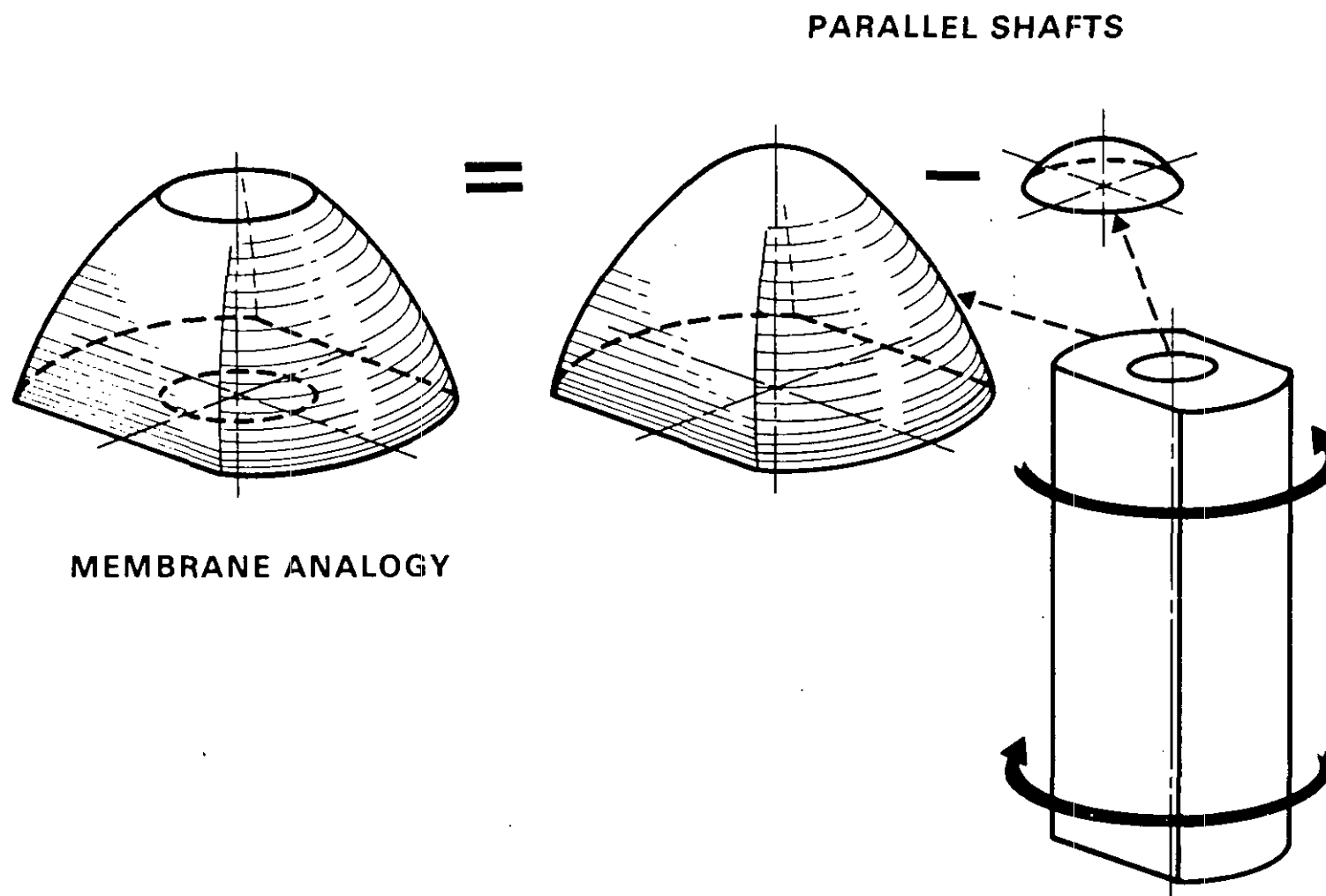
Figure 26. Parallel shaft concept.

56

DOUBLE BOUNDED REGION SOLUTION FOR HOLLOW SHAFTS
(Described in Appendix B)

PARALLEL SHAFTS CONCEPT

$R = 1.0$
$H/R = 0.3$
$V = 0.4667$
$T = 2G\theta(V)R^4$
$T = 0.9334\ G\theta$

$r = 0.5$
$T = G\theta(J)$
$= G\theta(\frac{\pi r^4}{2})$
$(OR\ 2G\theta(\frac{\pi r^4}{4}))$
$T = 0.0982\ G\theta$

$V = 0.4016$
$T = 2G\theta(V)$
$T = 0.8032 G\theta$

$\sum T = (0.9334 - 0.0982)\ G\theta$
$= 0.8352\ G\theta$

3.98% Deviation
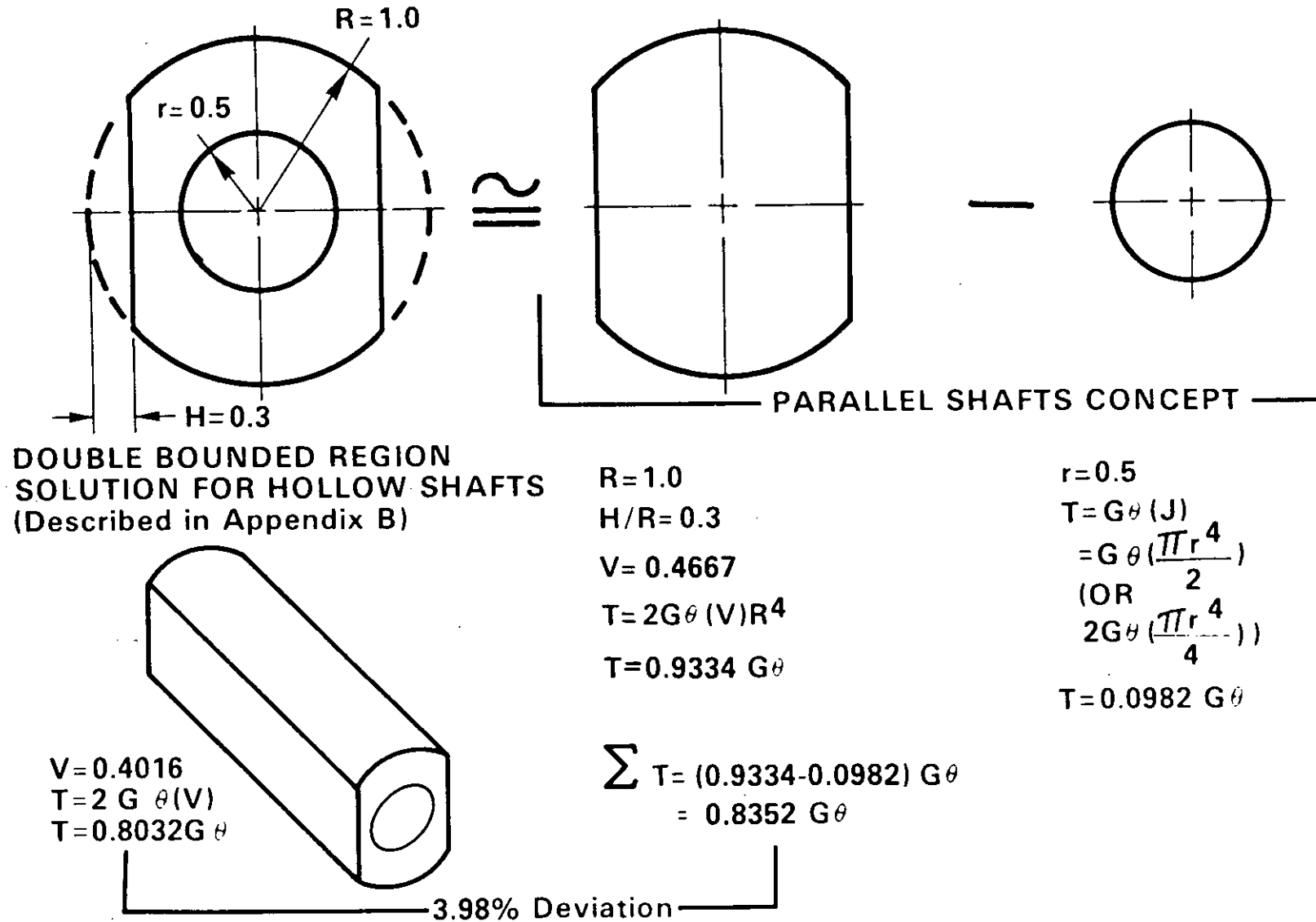
Figure 27. Milled shaft with central hole

57
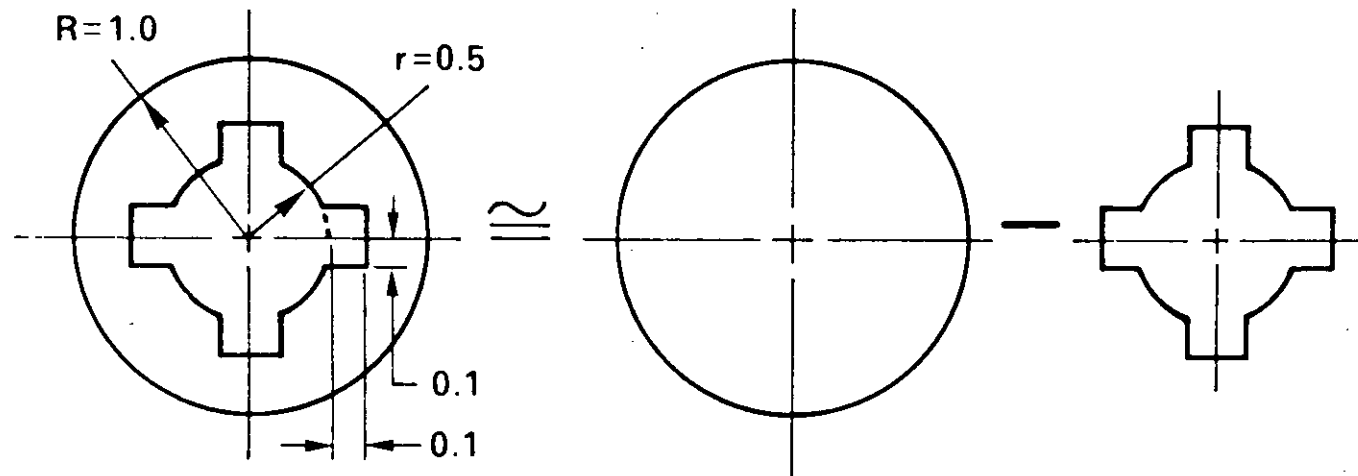
USING DOUBLE - BOUNDED
REGION COMPUTER SOLUTION

$V = 0.7104$

$T = 1.4208 \ (G)(\theta)$

USING CONCEPT OF SUPERPOSITION
OF PARALLEL SHAFTS

$V = 0.7854$

$T = 1.5708 \ (G)(\theta)$

$V = 0.8467(0.5)^4 = 0.0529$

$T = 0.1058 \ (G)(\theta)$

$\sum T = (1.5708 - 0.1058) \ (G)(\theta)$

$= 1.4650 \ (G)(\theta)$

3.11% Variation

Figure 28. Circular shaft with four inner splines

58

$$R = 1.0, A = B = 0.4, \quad \therefore A/B = 1.0, B/R = 0.4$$

$V = 0.9595$	$V = 0.8712$	$V = \pi/4 = 0.7854$
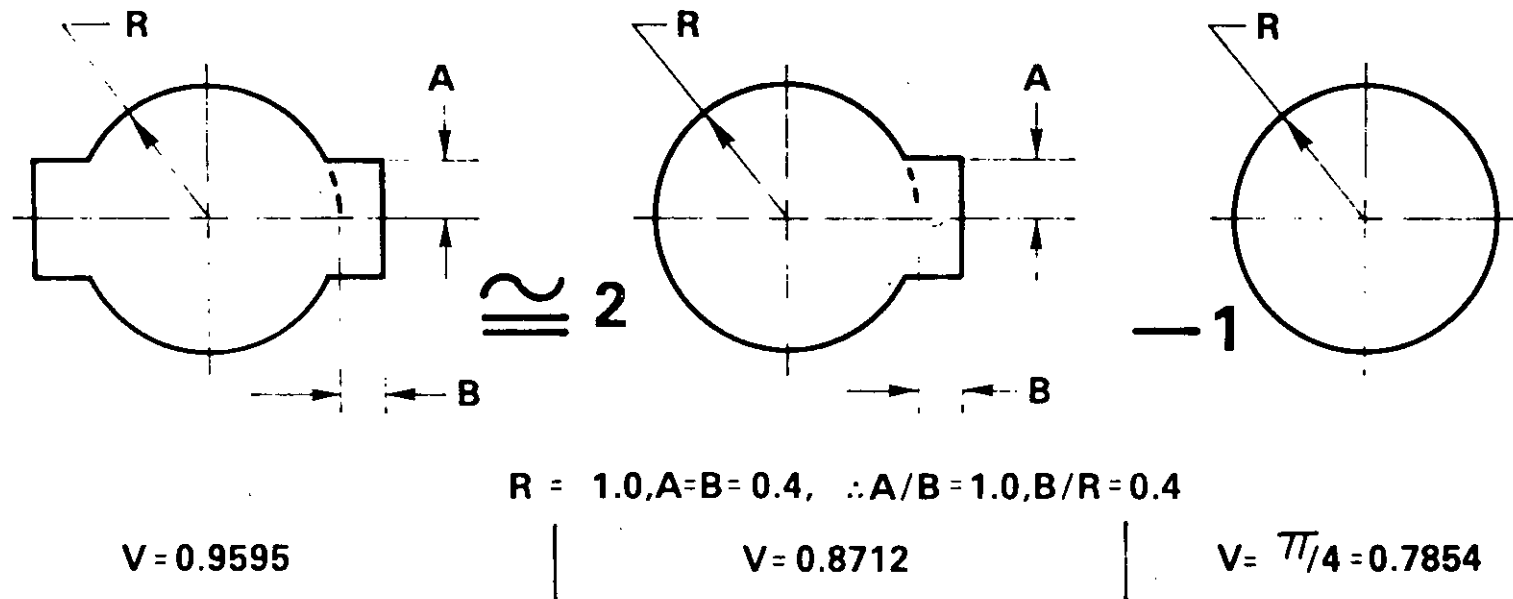
$$VR^4 = 0.9595(1)^4 \overset{?}{=} \sum VR^4 = 2(0.8712)(1)^4 - 0.7854(1)^4$$

$$0.9595 = (1.7424 - 0.7854) = 0.9570, \text{ a } 0.26\% \text{ VARIATION}$$

$$\text{(Table. 14)} \qquad \text{(Table. 12)}$$

$$f = \left(\frac{d\phi}{ds}/2V\right) = 0.5421 \overset{?}{=} \sum f = 2(0.5854) - \left(\frac{d\phi}{ds}/2V\right)$$

$$0.5421 = 1.1708 - (1/(2 \times .7854))$$

$$0.5421 = (1.1708 - .6366) = 0.5342$$

$$\text{a } 1.457\% \text{ VARIATION}$$

Figure 29. Superposition for two spline shaft

$$VR^4 = 0.9519\ (1)^4\ \stackrel{?}{=}\ 4.(0.8253)\ (1)^4 - 3\ (0.7854)\ (1)^4$$

$$0.9519\ =\ (3.3012 - 2.3562) = 0.945,\ \text{a } 0.72\%\ \text{VARIATION}$$

(Table. 16)   (Table. 12)

$$f = \left(\frac{d\phi}{ds}/2V\right) = 0.5720\ \stackrel{?}{=}\ 4(0.6120) - 3\left(\frac{d\phi}{ds}/2V\right)$$

$$0.5720\ =\ 2.448 - 3(1/(2x.7854))$$

$$0.5720\ =\ (2.448 - 1.9098) = 0.5382$$
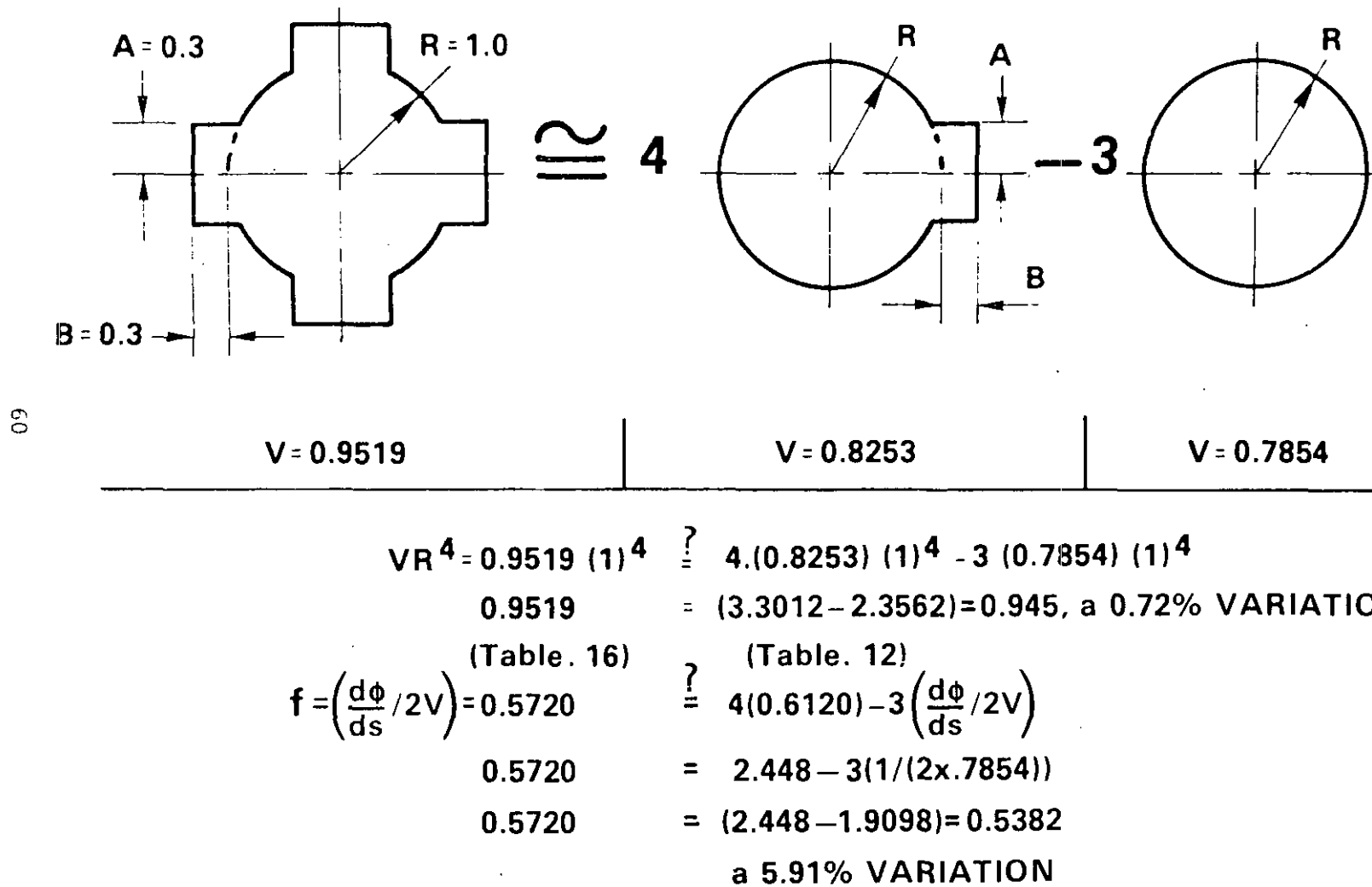
a 5.91% VARIATION

Figure 30. Superposition A for four spline shaft
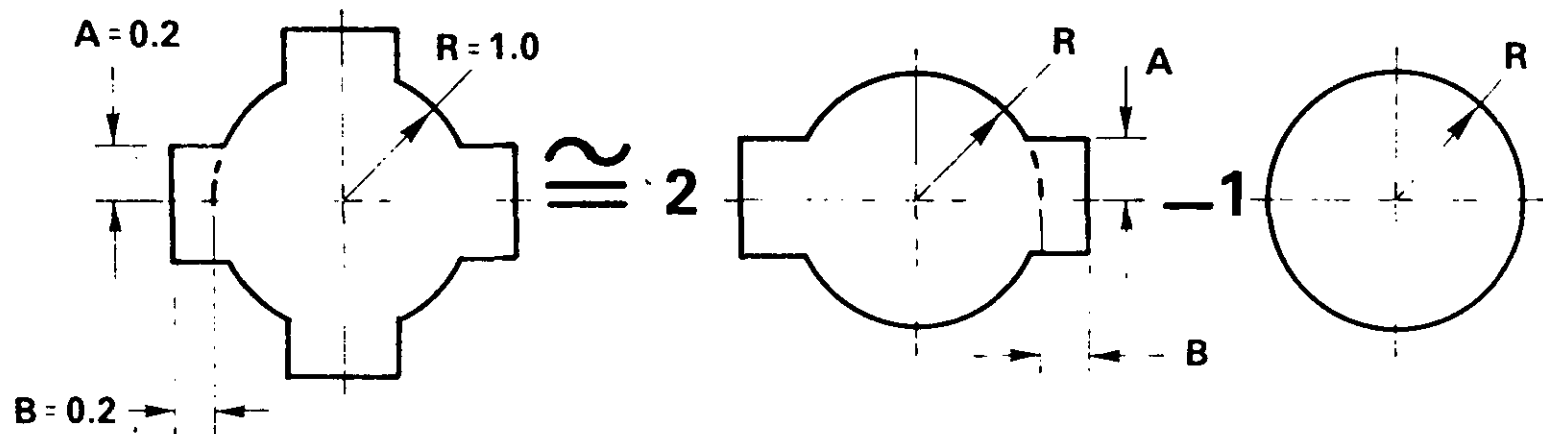
$$V = 0.8467 \qquad\qquad V = 0.8152 \qquad\qquad V = 0.7854$$

$$VR^4 = 0.8467(1)^4 \qquad \stackrel{?}{=} \qquad 2(0.8152)(1)^4 \qquad - \qquad (0.7854)(1)^4$$

$$0.8467 \qquad = \qquad (1.6304 - 0.7854) = 0.845, \text{ a } 0.2\% \text{ VARIATION}$$

$$\text{(Table . 16)} \qquad\qquad\qquad \text{(Table . 14)}$$

$$f = \left(\frac{d\phi}{ds}/2V\right) = 0.6109 \qquad \stackrel{?}{=} \qquad \sum f = 2(0.6184) - \left(\frac{d\phi}{ds}/2V\right)$$

$$0.6109 \qquad = \qquad 1.2368 - (1/(2 \times .7854))$$

$$0.6109 \qquad = \qquad (1.2368 - 0.6366) = 0.6002$$

$$\text{a } 1.75\% \text{ VARIATION}$$

Figure 31. Superposition B for four spline shaft

MIL-HDBK-776(AR)
15 September 1981

ILLUSTRATIVE DESIGN APPLICATION

Find the maximum torque that may be transmitted by the circular shaft with the interior splines (shown in Fig. 32) if the following design criteria are to be satisfied:

1) Maximum twist θ not to exceed 2 degrees over the full length of the shaft.

2) Maximum Shear Stress S_s not to exceed 15,000 kPa (psi)

Torque $T = \Sigma\ T = \Sigma\ 2G\theta(V)R^4 = 2G\theta\ \Sigma\ (V)R^4$

$\Sigma\ (V)R^4 = 0.7854-(0.1058-0.0491)$

$= 0.7854(1" \text{ circle})-0.0567(8 \text{ tooth spline})$

$= 0.7287$

Condition 1:

$\theta = 2\times(\pi/180)\times1/18) = 0.001939(\text{rad/in})$

$T = 2(12\times10^6)(0.001939)(0.7287) = 33,900(\text{in-lb})$

Condition 2:

S_s/T will be maximum at the outer contour, which is a complete circle (for which $d\phi/ds = 1.0$).

$S_s/T = G\theta(d\phi/ds)R/2G\theta\Sigma(VR^4))$

$= (d\phi/ds)R/2\Sigma(VR^4))$

$= (1.0)(1.0)/2(0.7287)) = 0.6862$

$T = S_s/0.6862 = 15,000/0.6862 = 21,860(\text{in-lb})$

Use T of 21,860(in lb) as maximum design Torque

62

$$VR^4 = (\pi/4)R^4$$
$$= (\pi/4)\ 1^4 = 0.7854$$

$$2V(R)^4 = 2(0.8468)(0.5)^4$$
$$= 0.1058$$

(From Table 15)

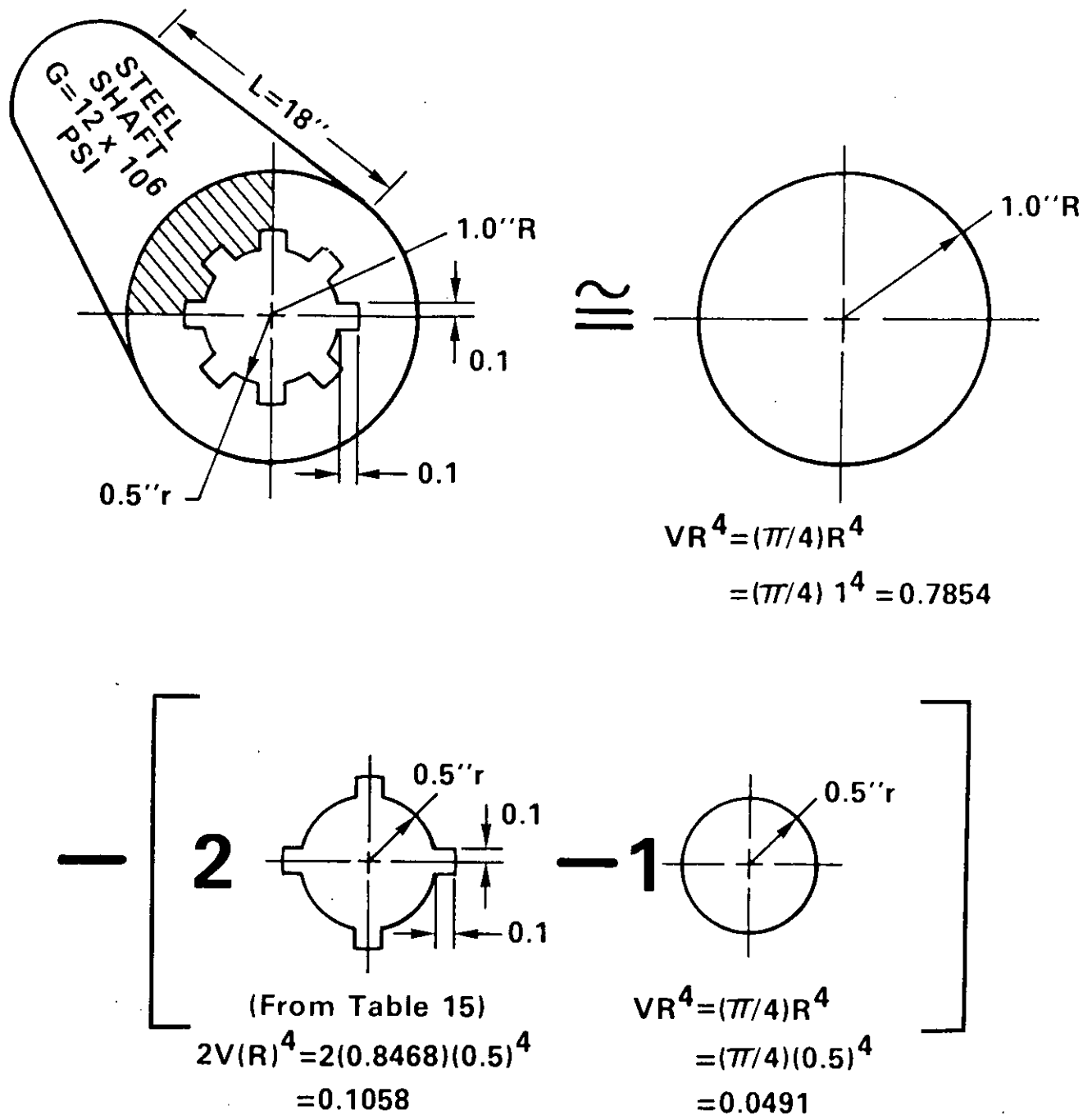$$VR^4 = (\pi/4)R^4$$
$$= (\pi/4)(0.5)^4$$
$$= 0.0491$$

Figure 32. Illustrative design application

63

MIL-HDBK-776(AR)
15 September 1981

(ANOTHER) ILLUSTRATIVE DESIGN APPLICATION

Find the maximum shear stress and angular twist per unit length produced by an imposed torque of 20,000 lb-in. The double milled steel shaft ($G=12 \times 10^6$ psi) has a 4-spline inner hole as shown (Figure 33).

OUTER CONTOUR: Double Milled Shaft

$$H/R = 0.1$$
V (Table 19) = 0.7149 (This is really $V(R)^4$ where R=1.0)
f (Table 20) = 0.8199

INNER CONTOUR: 4-Spline Shaft

$$A/B = 1.0, \quad B/R = 0.1/0.5 = 0.2$$
V (Table 15) = 0.8467 (Really $V(R)^4$ for a 1.0"R shaft)

$$T = 2.G.\Theta \Sigma V(R)^4$$

where $\Sigma V(R)^4 = 0.7149(1)^4 - 0.8467(0.5)^4$
$$= 0.6620$$

$$20,000 = 2 (12 \times 10^6)\Theta(0.6620)$$
and angular twist, $\Theta = 0.001259$ radians/inch

For a solid double-milled shaft, the maximum shear stress is at the midpoint of the flats:

$$S_S = T(f/R^3) = 20,000 \ (0.8199)/(1)^3$$
$$= 16,398 \text{ psi}$$

Because of the inner hole, however, the $V(R)^4$ term is reduced from 0.7149 to 0.6620. The maximum shear stress is still at the midpoint of the milled flats:

adjusted f'

$$S_S = T(f'/R^3) = 20,000 \ \left(0.8199 \times \frac{0.7149}{0.6620}\right) \Big/ (1)^3$$

$$= 17,708 \text{ psi}$$

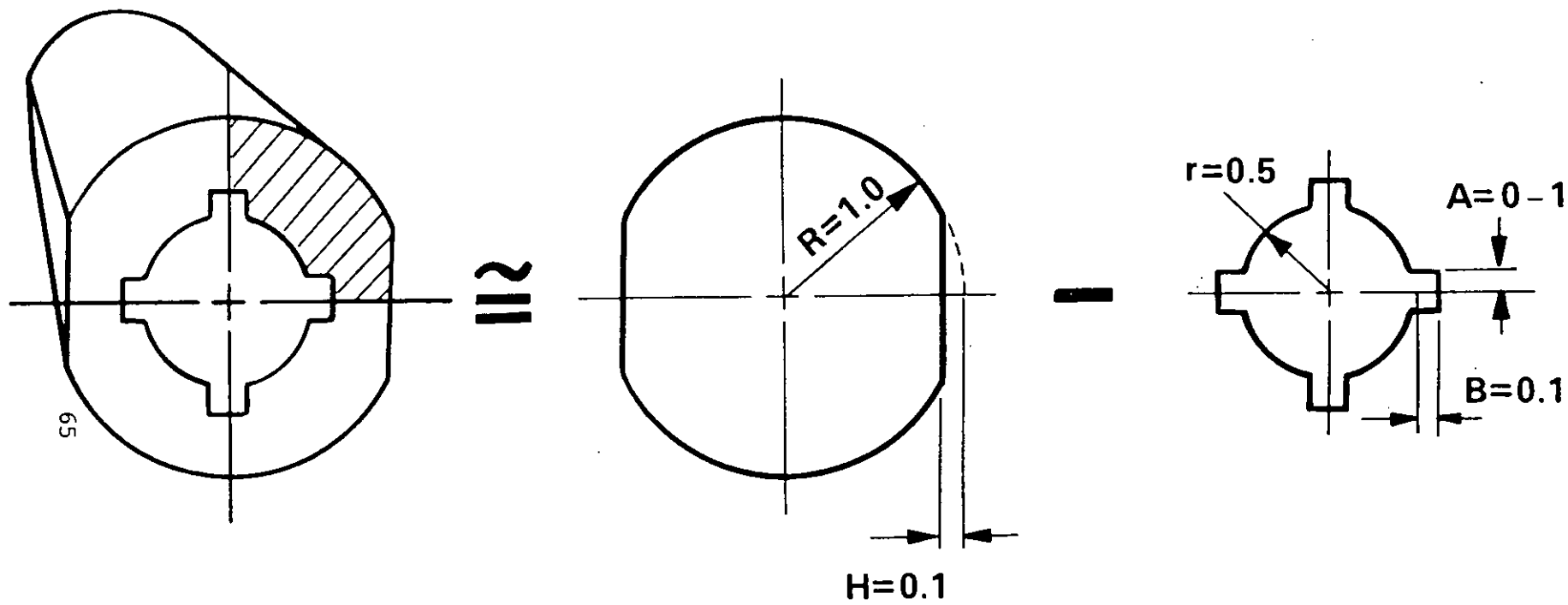The effect of the inner hole is to increase the maximum shear stress by 7.99%.

64

Figure 33.

MIL-HDBK-776(AR)
15 September 1981

BIBLIOGRAPHY

1. F. S. Shaw, "The Torsion of Solid and Hollow Prisms in the Elastic and Plastic Range by Relaxation Methods," Australian Council for Aeronautics, Report ACA-11, November 1944.

2. F. S. Shaw, An Introduction to Relaxation Methods, Dover Publications, Inc., Melbourne, Australia, 1953.

3. D. N. deG. Allen, Relaxation Methods, McGraw-Hill Book Company, Inc. New York, 1954.

4. D. H. Pletta and F. J. Maher, "The Torsional Properties of Round-Edged Flat Bars," Bulletin of the Virginia Polytechnic Institute, Vol XXXV, No. 7, Engineering Experiment Station Series No. 50, Blacksburg, Virginia, March 1942.

5. W. Ker Wilson, Practical Solution of Torsional Vibration Problems, Volume 1, 3rd Edition, John Wiley & Sons, Inc., New York, 1956.

6. R. I. Isakower and R. E. Barnas, "The Book of CLYDE - With a Torque-ing Chapter," U.S. Army ARRADCOM Users Manual MISD UM 77-3, Dover, NJ, October 1977.

7. R. I. Isakower and R. E. Barnas, "Torsional Stresses in Slotted Shafts," Machine Design, Volume 49, No. 21, Penton/IPC, Cleveland, Ohio, September 1977.

8. R.I. Isakower, "Design Charts for Torsional Properties of Non-Circular Shafts", U.S. Army Technical Report ARMID-TR-78001, Dover, NJ, November 1978.

APPENDIX A

MATHEMATICAL MODEL USED IN THE SHAFT COMPUTER PROGRAM

As the term implies, boundary value problems are those for which conditions are known at the boundaries. These conditions may be the value of the problem variable itself, the normal gradient or variable slope, or higher derivatives of the problem variable. For some problems, mixed boundary conditions may have to be specified: different conditions at different parts of the boundary. The SHAFT computer code solves those problems for which the problem variable itself (the stress function) is known at the boundary.

Given sets of equally spaced arguments and corresponding tables of function values, the finite difference analyst can employ forward, central, and backward difference operators. SHAFT is based upon central difference operators which approximate each differential operator in the partial differential equation (PDE).

The problem domain is overlayed with an appropriately selected grid. There are many shapes (and sizes) of overlaying Cartesian and polar coordinate grids:

    rectangular
    square
    equilateral-triangular
    equilangular-hexagonal
    oblique

Throughout the area of the problem, SHAFT uses a constant-size square grid for which the percentage errors are of the order of the grid size squared (h^2). This grid (or net) consists of parallel vertical lines spaced h units apart, and parallel horizontal lines, also spaced h units apart, which blanket the problem area from left-to-right and bottom-to-top.

The intersection of the grid lines with the boundaries of the domain are called boundary nodes. The intersections of the grid lines with each other within the problem domain are called inner domain nodes. It is at these inner domain nodes that the finite difference approximations are applied. The approximation of the partial differential equation with the proper finite difference operators replaces the PDE with a set of subsidiary linear algebraic equations, one at each inner domain node. In practical applications, the method

67

must be capable of solving problems whose boundaries may be curved. In such cases, boundary nodes are not all exactly h units away from an inner node, as is the case between adjacent inner nodes. The finite difference approximation of the harmonic operator at each inner node involves not only the variable value of that node and at the four surrounding nodes (above, below, left, and right), but also the distance between these four surrounding nodes and the inner node. At the boundaries, these distances vary unpredictably. Compensation for the variation must be included in the finite difference solution. SHAFT represents the problem variable by a second-degree polynomial in two variables, and employs a generalized irregular "star" in all directions for each inner node. In practice, one should avoid a grid so coarse that more than two arms of the star are irregular (or less than h units in length). The generalized star permits, and automatically compensates for, a variation in length of any of the four arms radiating from a node. For no variation in any arm, the algorithm reduces exactly to the standard harmonic "computation stencil".

At each inner domain node, a finite difference approximation to the governing partial differential equation (PDE) is generated by SHAFT. The resulting set of linear algebraic equations is solved simultaneously by the program for the unknown problem variable (stress function) at each node in the overlaying finite difference grid. A graphics version of the program also generates, and displays on the CRT screen, iso-value contour maps for any desired values of the variable. This way, a more meaningful picture of the solution in the form of stress concentration contour lines of different values is made available to the engineer.
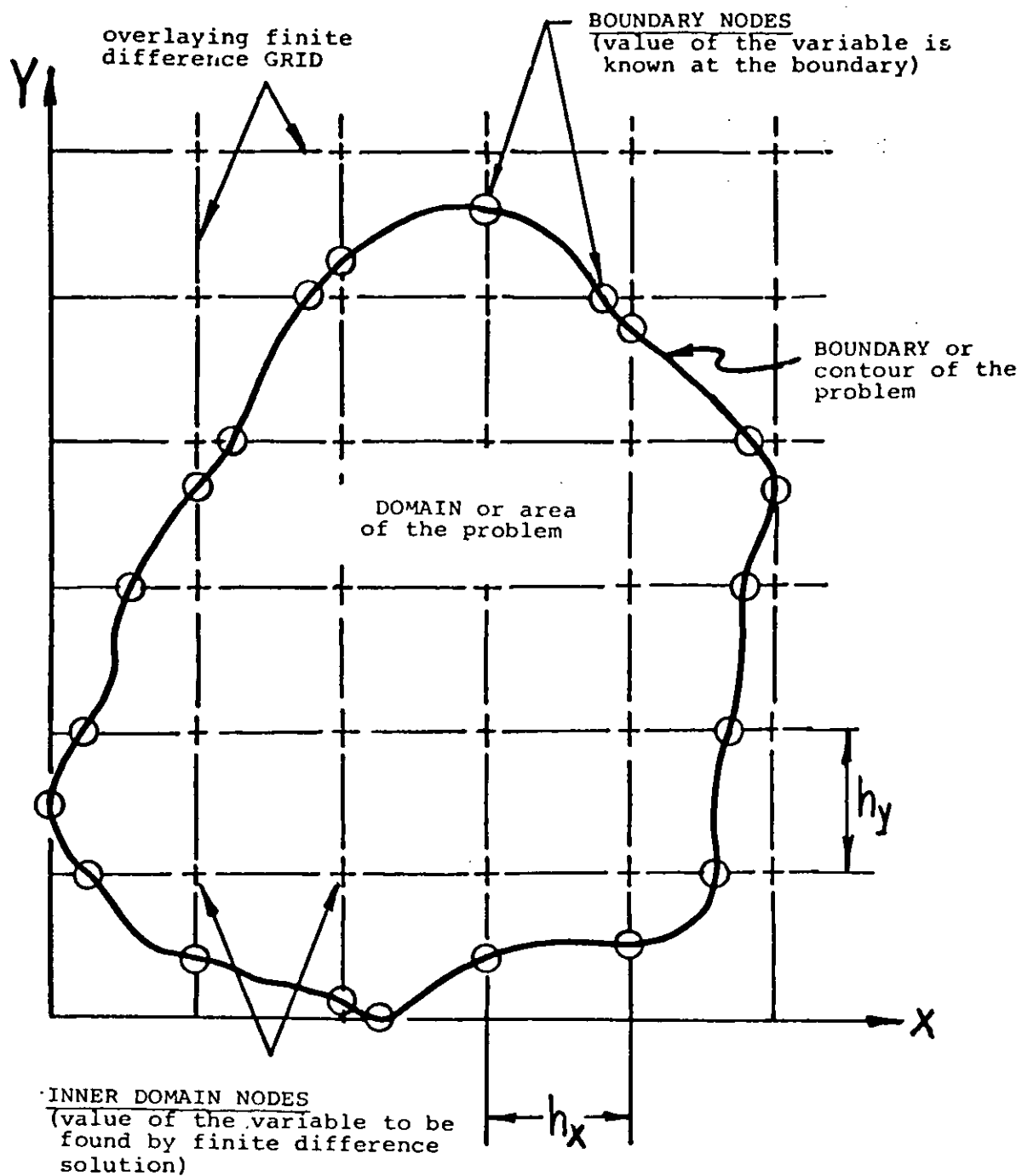
Figure A-1. Finite difference grid.

If the problem geometry is symmetrical, the designer does not have to display and work with the entire picture of the problem, he need only work with the "repeating section". In essence, the graphics user may examine the problem solution at will and redesign the problem (contour, boundary conditions, equation coefficients, etc.) at the screen re-solving the "new design" problem.

Consider the general expression:

Where A,B,D are arbitrary constants.

$$\nabla^2 f = A \frac{\partial^2 f}{\partial x^2} + B \frac{\partial^2 f}{\partial y^2} = D$$

Using central differences, the finite difference approximations to the partial differential operators of function f at representative node 0 are:

$$\frac{\partial f}{\partial x} = \frac{1}{2h_x} (f_1 - f_3), \quad \frac{\partial f}{\partial y} = \frac{1}{2h_y} (f_2 - f_4)$$

$$\frac{\partial^2 f}{\partial x^2} = \frac{1}{h_x^2} (f_1 - 2f_0 + f_3)$$

$$\frac{\partial^2 f}{\partial y^2} = \frac{1}{h_y^2} (f_2 \ 2f_0 + f_4)$$

for a square grid $h_x = h_y = h$ and the harmonic operator $\nabla^2 f$ becomes:

$$h^2 \nabla^2 f_0 = [A (f_1 + f_3) + B (f_2 + f_4) - (A+B) 2f_0] = h^2 D$$

70

COMPUTATION STENCIL
AT NODE O

FOR

$$\nabla^2 f = A \frac{\partial^2 f}{\partial X^2} + B \frac{\partial^2 f}{\partial Y^2} = D$$
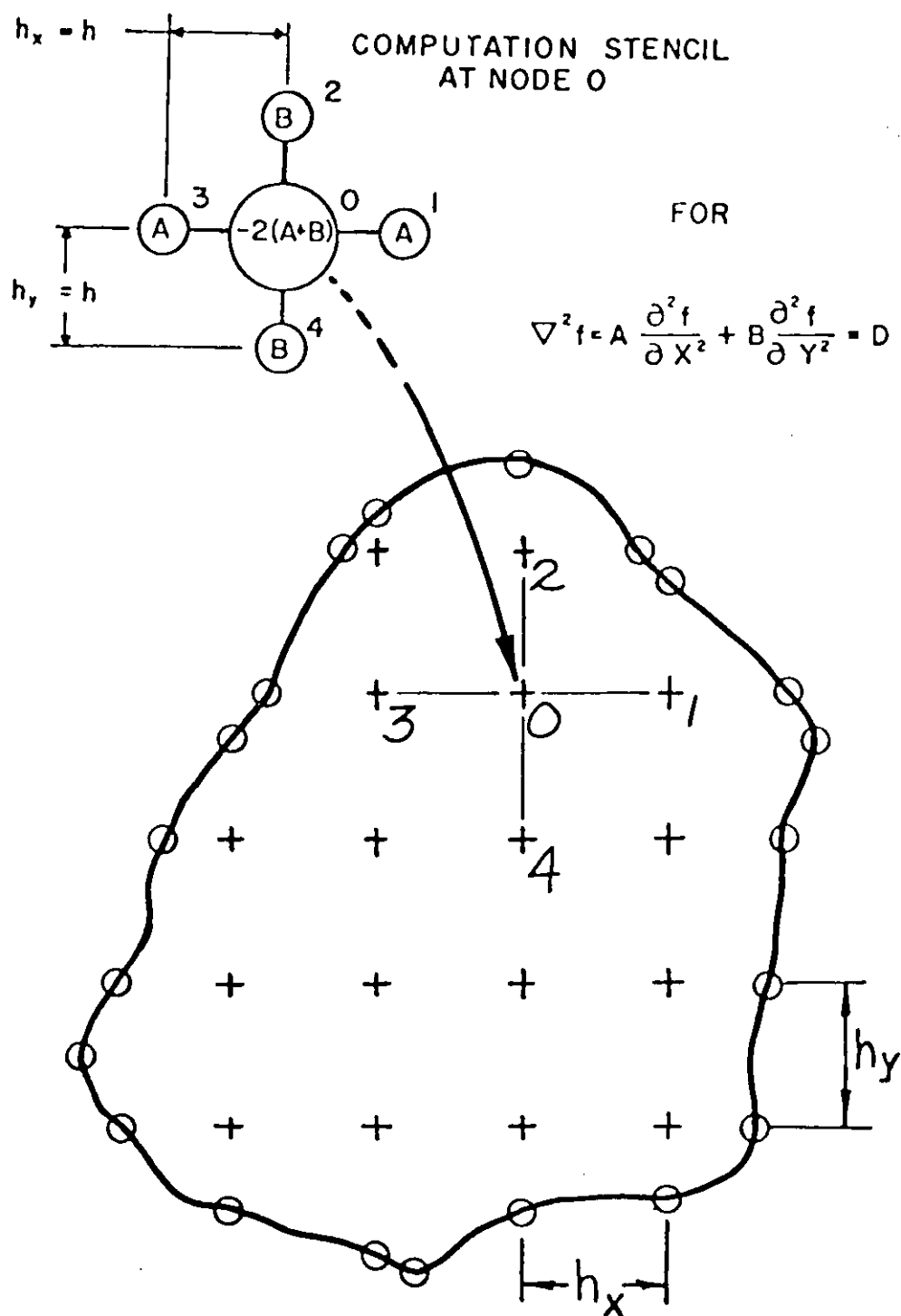
Figure A-2.   Harmonic operator for square star in X-Y grid.

71

This finite difference equation at node zero involves the unknown variable at node zero (f_0) plus the unknown value of the variable at the four surrounding nodes (f_1, f_2, f_3, f_4), plus the grid spacing (h). The five nodes involved form a four-arm star with node zero at the center. This algebraic (or difference) equation could be conveniently visualized as a four-arm computation stencil made up of five "balloons" connected in a four-arm star pattern and overlayed on the grid nodes. The value within each balloon is the coefficient by which the variable (f) at that node is multiplied to make up the algebraic approximation equation.

The numerical treatment of an irregular star ($h_1 \neq h_2 \neq h_3 \neq h_4$) represents the function f near the representative node O by a second-degree polynomial in X and Y:

$$f(X,Y) = f_0 + a_1 X + a_2 Y + a_3 X^2 + a_4 Y^2 + a_5 XY$$

Evaluating this polynomial at the neighboring nodes (1, 2, 3, 4) produces the following set of equations:

$$f_1 = f_0 + a_1 h_1 + a_3 h_1{}^2$$

$$f_2 = f_0 + a_2 h_2 + a_4 h_2{}^2$$

$$f_3 = f_0 - a_1 h_3 + a_3 h_3{}^2$$

$$f_4 = f_0 - a_2 h_4 + a_4 h_4{}^2$$

which are tnen solved for a_3 and a_4 which are necessary to satisfy the harmonic operator $\nabla^2 f$, since:

$$\frac{\partial f}{\partial x} = a_1 + 2a_3 X + a_5 Y, \quad \frac{\partial^2 f}{\partial x^2} = 2a_3$$

$$\frac{\partial f}{\partial y} = a_2 + 2a_4 Y + a_5 X, \quad \frac{\partial^2 f}{\partial y^2} = 2a_4$$

and

$$\nabla^2 f = A (2a_3) + B (2a_4)$$

72

Performing the necessary algebraic operations, substituting results, collecting terms, and using the following ratios:

$$b_1 = \frac{h_1}{h} \qquad b_2 = \frac{h_2}{h}$$

$$b_3 = \frac{h_3}{h} \qquad b_4 = \frac{h_4}{h}$$

The harmonic operator becomes:

$$h^2 \nabla^2 f_0 = \left[\frac{2A}{b_1(b_1+b_3)} f_1 + \frac{2B}{b_2(b_2+b_4)} f_2 + \right.$$

$$+ \frac{2A}{b_3(b_1+b_3)} f_3 + \frac{2B}{b_4(b_2+b_4)} f_4 +$$

$$\left. - \left(\frac{2A}{b_1 b_2} + \frac{2B}{b_2 b_4} \right) f_0 \right] = h^2 D$$

IRREGULAR STAR AT NODE 0
&
NEIGHBORING NODES (1, 2, 3, 4,)

$$b_i = h_i/h$$

$$\frac{2B}{b_2(b_2 + b_4)}$$

$$\frac{2A}{b_3(b_1 + b_3)}$$

$$-\left(\frac{2A}{b_1 b_3} + \frac{2B}{b_2 b_4}\right)$$

$$\frac{2A}{b_1(b_1 + b_3)}$$

COMPUTATION STENCIL
AT NODE 0

$$\frac{2B}{b_4(b_2 + b_4)}$$

FOR

$$\nabla^2 f = A\frac{\partial^2 f}{\partial x^2} + B\frac{\partial^2 f}{\partial Y^2} = D$$
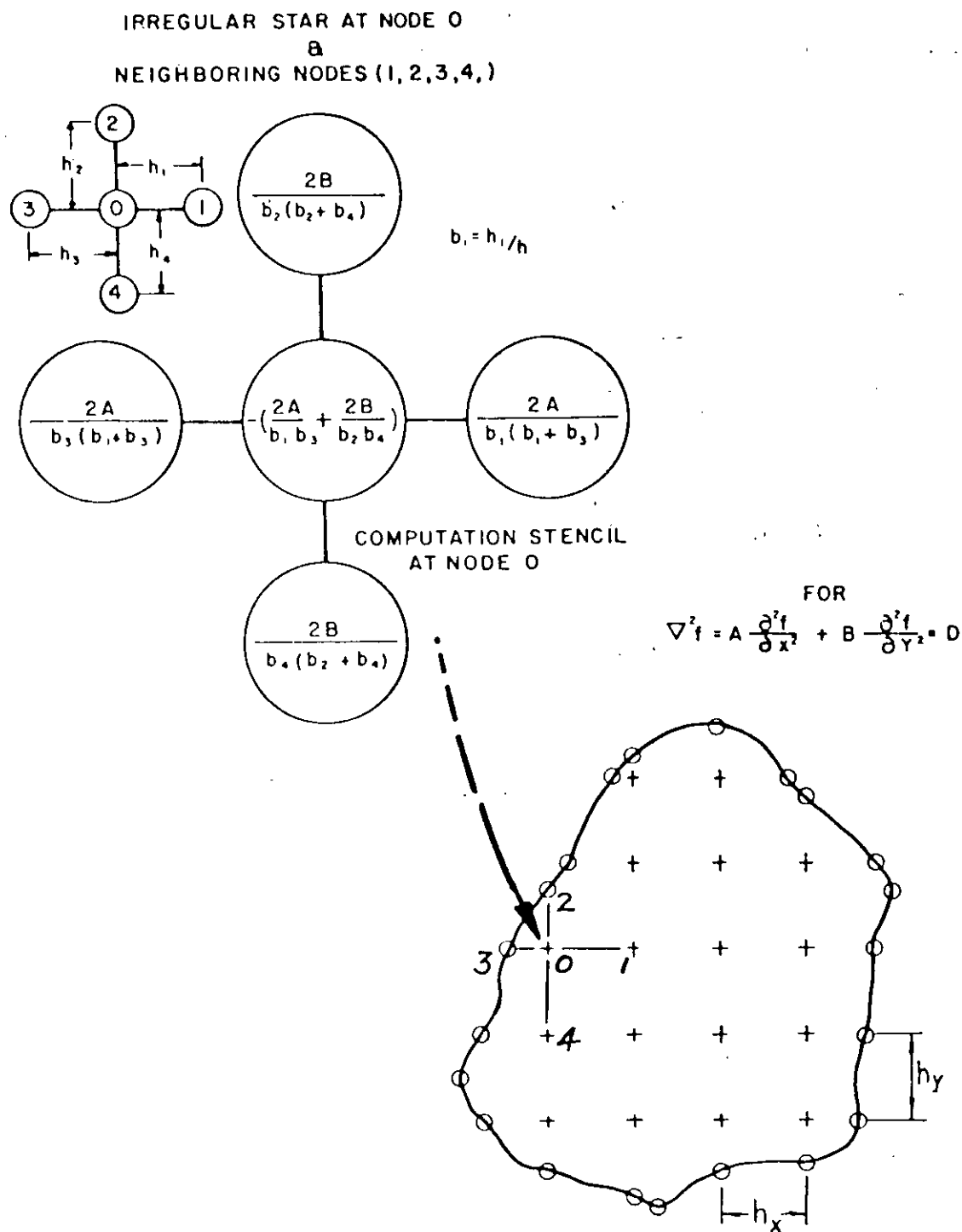
Figure A-3.   Harmonic operator for irregular star in X-Y grid.

APPENDIX B

EXTENSION OF MODEL TO HOLLOW SHAFTS

This would appear to be a simple matter of solving the governing PDE over a multiply-connected boundary, were it not for the uncertainty concerning boundary conditions. The actual value of the problem variable at the boundary was not important in the torsion application, only the difference in the problem variable at various points mattered. The problem variable at the boundary could be assumed to have any value, as long as there was only one boundary. With two or more boundaries the solution calls for a different approach.

The stress function is obtained as the superposition of two solutions, one of which is adjusted by a factor (k). This is the programmed solution to shafts with a hole. The hole may be of any shape, size, and location. The two solutions, to be combined, are shown in figure B-1: equations and boundary conditions. Once the contour integrals are taken around the inner boundary of area A_B, the only unknown, k, may be readily obtained. The contour integral, which need not be evaluated around the actual boundary, may be taken around any contour that encloses that boundary, and includes none other (for example, see shaded area A_B) in figure B-1.

---

[1] F.S. Shaw, The Torsion of Solid and Hollow Prisms in the Elastic and Plastic Range by Relaxation Methods, Australian Council for Aeronautics, Report ACA-11, November 1944, pp 8,11,23.
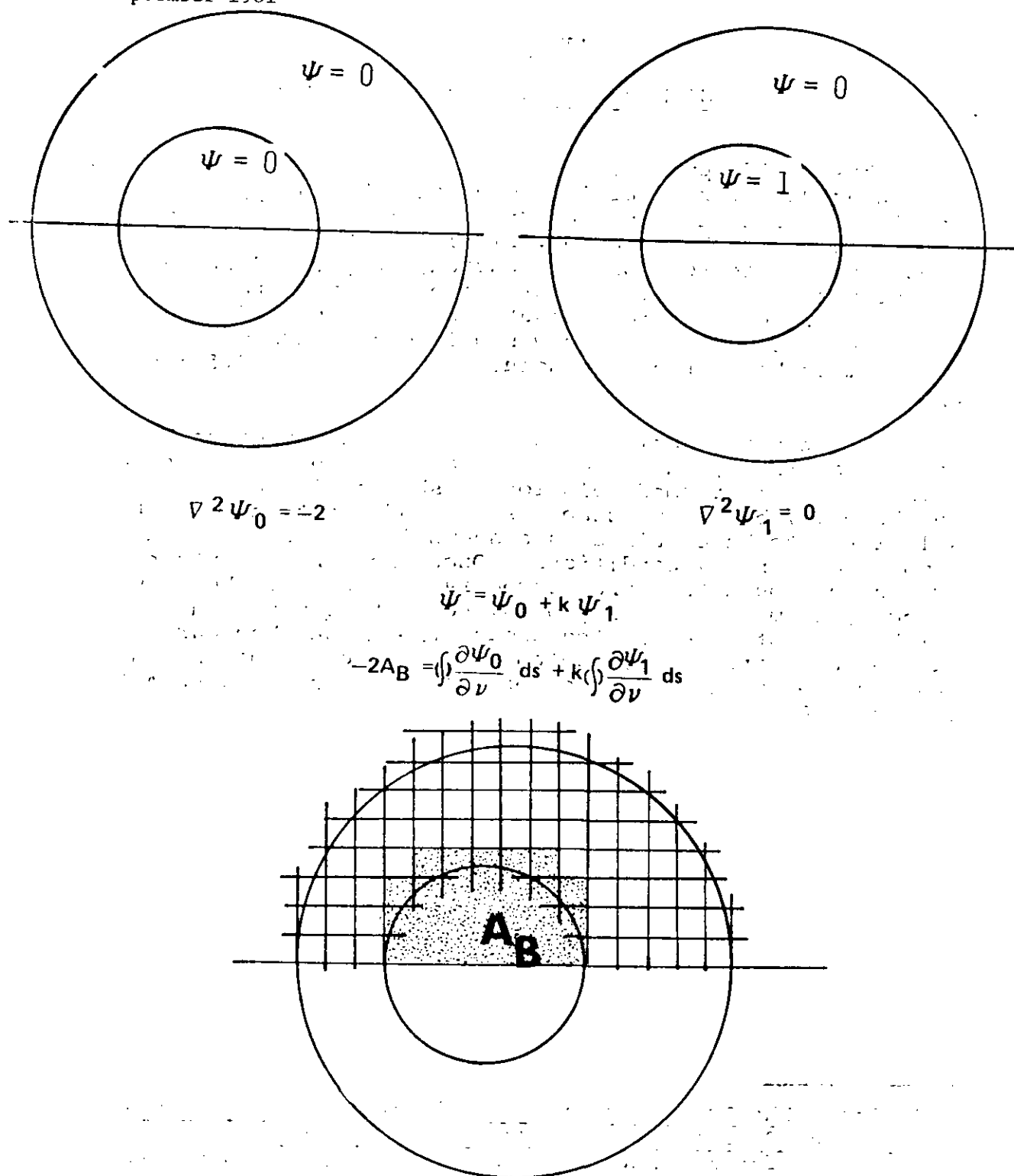
$$\psi = 0$$

$$\psi = 0$$

$$\psi = 0$$

$$\psi = 1$$

$$\nabla^2 \psi_0 = -2$$

$$\nabla^2 \psi_1 = 0$$

$$\psi = \psi_0 + k\psi_1$$

$$-2A_B = \oint \frac{\partial \psi_0}{\partial \nu}\, ds + k \oint \frac{\partial \psi_1}{\partial \nu}\, ds$$

$$A_B$$

Figure B-1. Mathematical approach to hollow shaft problem.

76

Custodian:
   Army - AR

User activity:
   Navy - OS

Review activities
   Army - AV, ME

Preparing activity:
   Army - AR

Project Number: CDNC-0012

STANDARDIZATION DOCUMENT IMPROVEMENT PROPOSAL

INSTRUCTIONS: This form is provided to solicit beneficial comments which may improve this document and enhance its use. DoD contractors, government activities, manufacturers, vendors, or other prospective users of the document are invited to submit comments to the government. Fold on lines on reverse side, staple in corner, and send to preparing activity. Attach any pertinent data which may be of use in improving this document. If there are additional papers, attach to form and place both in an envelope addressed to preparing activity. A response will be provided to the submitter, when name and address is provided, within 30 days indicating that the 1426 was received and when any appropriate action on it will be completed.

NOTE: This form shall not be used to submit requests for waivers, deviations or clarification of specification requirements on current contracts. Comments submitted on this form do not constitute or imply authorization to waive any portion of the referenced document(s) or to amend contractual requirements.

DOCUMENT IDENTIFIER (Number) AND TITLE

MIL-HDBK-776(AR) Shafts, Elastic Torsional Stress Analysis Of

NAME OF ORGANIZATION AND ADDRESS OF SUBMITTER

☐ VENDOR   ☐ USER   ☐ MANUFACTURER

1. ☐ HAS ANY PART OF THE DOCUMENT CREATED PROBLEMS OR REQUIRED INTERPRETATION IN PROCUREMENT USE? ☐ IS ANY PART OF IT TOO RIGID, RESTRICTIVE, LOOSE OR AMBIGUOUS? PLEASE EXPLAIN BELOW.

A. GIVE PARAGRAPH NUMBER AND WORDING

B. RECOMMENDED WORDING CHANGE

C. REASON FOR RECOMMENDED CHANGE(S)

2. REMARKS

SUBMITTED BY (Printed or typed name and address — Optional)

TELEPHONE NO.

DATE

DD FORM 1426
1 OCT 76

EDITION OF 1 JAN 72 WILL BE USED UNTIL EXHAUSTED.